DUAL BAND OCTAGONAL MICROSTRIP PATCH ANTENNA DESIGN METHOD FOR ENERGY HARVESTING

by

Francisco A. Rivera-Abreu

A Thesis

Submitted to the Faculty of Purdue University

In Partial Fulfillment of the Requirements for the degree of

Master of Science in Electrical Engineering

Department of Electrical and Computer Engineering

Fort Wayne, Indiana

December 2018

THE PURDUE UNIVERSITY GRADUATE SCHOOL
STATEMENT OF COMMITTEE APPROVAL

Dr. Abdullah Eroglu, Chair

     Department of Electrical and Computer Engineering

Dr. David Cochran

     Department of Electrical and Computer Engineering

Dr. Chao Chen

     Department of Electrical and Computer Engineering

Approved by:

     Dr. Abdullah Eroglu

          Head of the Graduate Program

Dedicated to Marisarah

ACKNOWLEDGMENTS

TABLE OF CONTENTS

LIST OF TABLES

LIST OF FIGURES

LIST OF ABBREVIATIONS

VSWR   Voltage Standing Wave Ratio

RL   Return Loss

RP   Radiation Pattern

OMPA   Octagonal Microstrip Patch Antenna

HFSS   High Frequency Simulation Structure

EOA   Elevation Over Azimuth

EM   Electromagnetic

ABSTRACT

Author: Rivera-Abreu, Francisco A. Master of Science in Engineering
Institution: Purdue University
Degree Received: December 2018
Title: Dual Band Octagonal Microstrip Antenna Design Method for Energy Harvesting
Major Professor: Dr. Abdullah Eroglu

With the rapid growth of wireless systems and demands of low-power integrated electronic circuits, various research works have been implemented to study the practicability of powering these systems and circuits by harvesting ambient electromagnetic (EM) energy (free energy). Microstrip antennas are the most rapidly developing field in last thirty years. Currently these antennas are applied in mobile radio systems, integrated antennas, satellite navigation receivers, satellite communications, direct broadcast radio and television, etc. The considerable interest in the microstrip antennas is due to their advantages compared to the conventional microwave antenna as lightweight, low volume, conformability, and ease of fabrication. In this paper, a dual-band microstrip patch antenna is designed to radiate at 900 MHz and 1.8 GHz. Two rectangular microstrip patch antennas were designed for the two frequencies of interest. After designing the two rectangular microstrip antennas, their length and width were combined to design the dual band octagonal microstrip patch antenna. The antenna consists of two dielectric substrate layers that are stacked together. On the first layer, the octagonal patch is etched. The second layer is the feed layer with a proximity coupling feed and in the bottom the ground plane. The material used for the dielectric is Rogers TMM 10i with a dielectric constant ε_r of 9.8 and thickness of 1.6 mm. The proposed antenna can be used to harvest the energy from Wi-Fi and widely spread mobile networks. The octagonal microstrip patch antenna was designed by the software ANSYS Electronics Desktop 2017. The simulated and measured results show good agreement. The proposed dual band antenna has good bandwidth, gain and radiation characteristics at the frequency of interests. It has also lower profile in comparison to conventional microstrip patch antennas. One additional simulation of the octagonal antenna for 2.4 GHz was realized to prove that the method works. In the future, mobile devices will be able to recharge itself by using microstrip antennas for energy harvesting.

1. INTRODUCTION

With the rapid growth of wireless systems and demands of low-power integrated electronic circuits, various research works have been implemented to study the practicability of powering these systems and circuits by harvesting ambient electromagnetic (EM) energy (free energy) [1]–[4].

Microstrip antennas are the most rapidly developing field in last thirty years. Currently these antennas are applied in mobile radio systems, integrated antennas, satellite navigation receivers, satellite communications, direct broadcast radio and television, etc. The considerable interest in the microstrip antennas is due to their advantages compared to the conventional microwave antenna as lightweight, low volume, conformability, and ease of fabrication [7]. Nevertheless, the microstrip antennas typically suffer from narrowband radiation (a few percent of center frequency), low gain, tolerance problem and limited power capacity.

Now, with the development of microwave integrated technology and wireless communication technology, it needs the transceiver equipment can work in different frequency bands. The systems such as the satellites, the global position system (GPS) are normal required to operate at two different frequencies. Using of the microstrip antennas can be instead of the use of two different single band antennas. Variety of methods has been proposed to obtain dual frequency operation. Among them, loading slits [8], loading the patch with shorting pins [9]-[11], using slots in the patch [12-13], using stacked patches, or using two feeding ports [14] are the mostly exploited ones. Pozar [15] proposed a new feeding technique for microstrip antennas based on the coupled-aperture concept in order to achieve a large bandwidth. The technique consists of coupling energy from the strip-line though an aperture in the ground plane. The radiating element is isolated from the feed network by the ground plane, which minimizes spurious radiation, and gives the designer the possibility to select independent substrate materials for the feed and the patch.

1.1   Microstrip Antenna

Microstrip antennas (often called patch antennas) are widely used in the microwave frequency region because of their simplicity and compatibility with printed-circuit technology, making

them easy to manufacture either as stand-alone elements [16]. Microstrip patch antennas designs consist generally of four parts (patch layer, ground plane layer, substrate, and the feeding port) as shown in Figure 1.1.
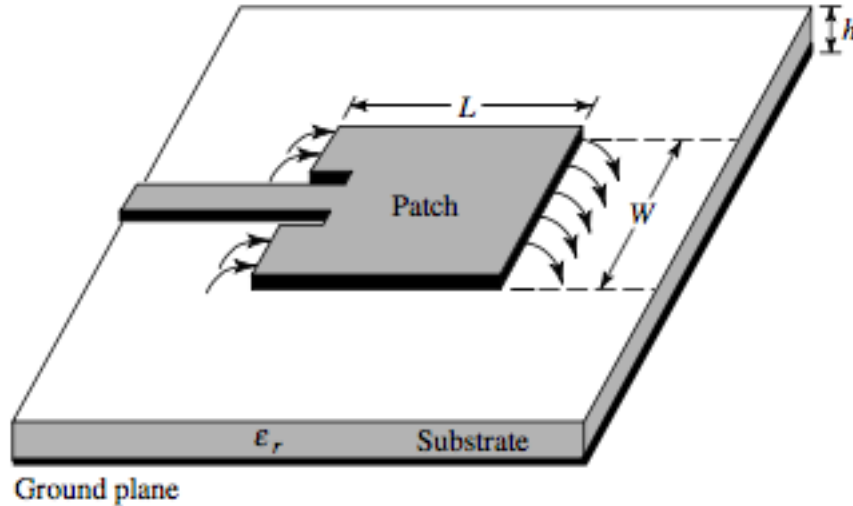
Figure 1.1 Microstrip Antenna

The patch layer is very thin (t<<λ0, where λ0 is the free space wavelength). radiating metal strip located on one side of a thin no conducting substrate, the ground plane is the same metal located on the bottom of the substrate. The metallic patch is normally made of thin copper. Many shapes of patches are designed some are shown in Figure 1.2 and the most popular shape is the rectangular and circular patch. The substrate layer thickness is 0.01–0.05 of free-space wavelength (λ_0). It is used primarily to provide proper spacing and mechanical support between the patch layer and its ground plane. It is also often used with high dielectric-constant material to load the patch and reduce its size. The substrate material should be low in insertion loss with a loss tangent of less than 0.005. In this work we have used TMM 10i with dielectric constant εr of 9.8 and tangent loss of 0.002. Generally, substrate materials can be separated into three categories according to the dielectric constant εr [16]: (1) Having a relative permittivity εr in the range of 1.0–2.0 this type of material can be air, polystyrene foam, or dielectric honeycomb, (2) Having ε_r in the range of 2.0 to 4.0 with material consisting mostly of fiberglass reinforced Teflon and (3) With an εr between 4 and 10 the material can consist of ceramic, quartz, or alumina. The advantages of the microstrip antennas are small size, low profile, and lightweight,

conformable to planar and non-planar surfaces [17]. It demands a very little volume of the structure when mounting. They are simple and cheap to manufacture using modern printed-circuit technology [17]. However, patch antennas have disadvantages. The main disadvantages of the microstrip antennas are: low efficiency, narrow bandwidth of less than 5%, low RF power due to the small separation between the radiation patch and the ground plane (not suitable for high-power applications) [17].

1.2 Type of Patch Antennas

The radiating patch may be square, rectangular, thin strip (dipole), circular, elliptical, triangular, or any other configuration. These and others are illustrated in Figure 1.2. Square, rectangular, dipole (strip), and circular are the most common because of ease of analysis and fabrication, and their attractive radiation characteristics, especially low cross-polarization radiation [17]. Thickness of the substrate h has a big effect on the resonant frequency fr and bandwidth BW of the antenna.

(a) Square (b) Rectangular (c) Dipole (d) Circular (e) Elliptical

(f) Triangular (g) Disc sector (h) Circular ring (i) Ring sector
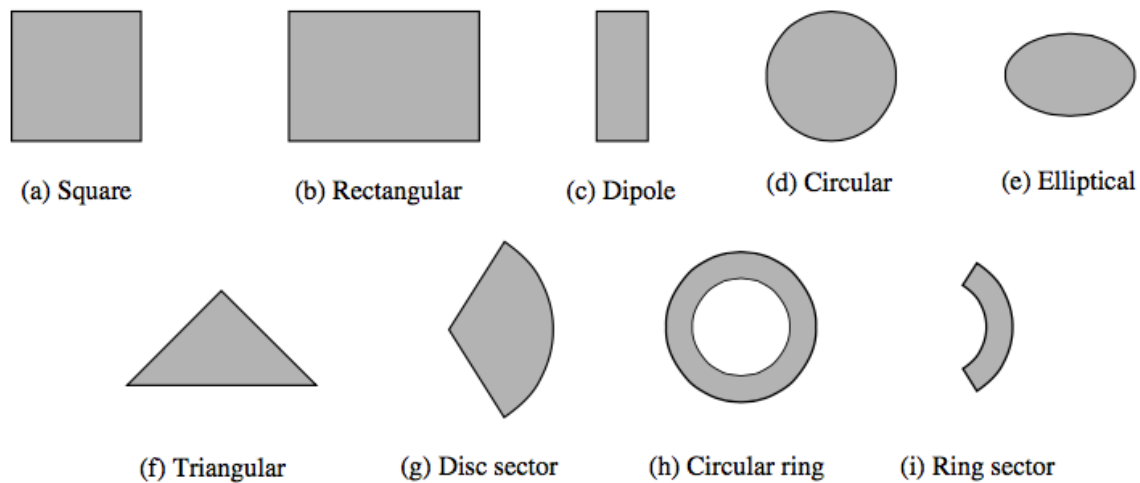
Figure 1.2 Representative shapes of microstrip patch.

1.3 Feeding Methods

There are many configurations that can be used to feed microstrip antennas. The four most popular are the microstrip line, coaxial probe, aperture coupling, and proximity coupling [19]-

[26]. These are displayed in Figure 1.3. The selection of the feeding method is based on its efficiency power transfer between the radiating patch and the feed line that is the impedance matching between them. Basically, they can be classified into two categories; the contacting and non-contacting method. In the contacting method, the RF source is fed directly to the radiating patch using a connecting element such as a microstrip line. In the non-contacting method, electromagnetic field coupling is done to transfer power between the microstrip line and the radiating patch. Below is some most popular feeding technique. In this work we have used the proximity coupling.

a) Microstrip Line Feed

b) Aperture Coupling

c) Coaxial Probe

d) Proximity Coupling
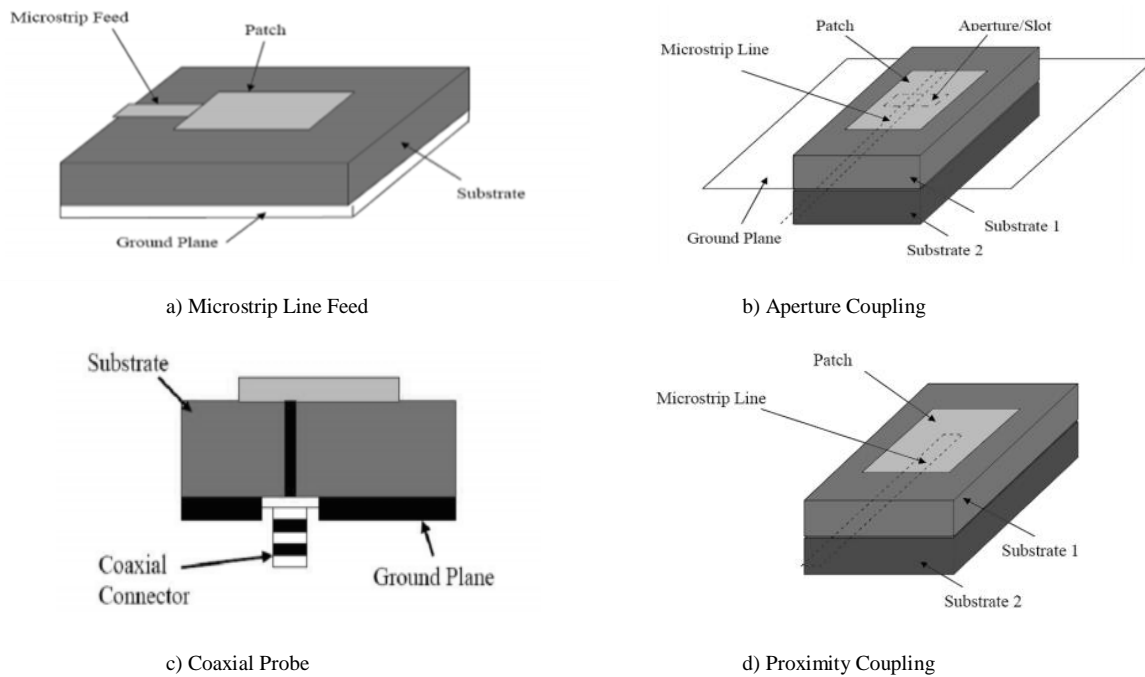
Figure 1.3 Typical feeds for microstrip antennas.

1.3.1   Microstrip Line Feed

The microstrip feed line is also a conducting strip, usually of much smaller width compared to the patch. The microstrip-line feed is easy to fabricate, simple to match by controlling the inset position and rather simple to model [17]. The width and the inset position of the strip line can be optimized to match the input impedance without the need for any additional matching element. This provides an ease in term of fabrication, modeling and the impedance matching. However, as the thickness of the dielectric substrate is increased, surface waves and spurious feed radiation also increases, creating a limit to the bandwidth of the antenna [5].
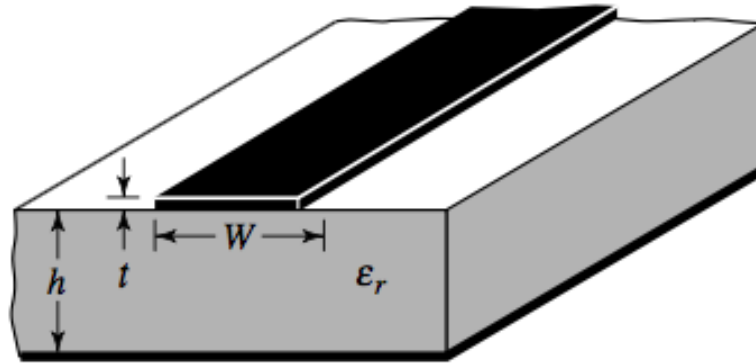
Figure 1.4 Microstrip Feed Line

1.3.2 Proximity Coupling

As shown in Figure 1.5, the feed line is sandwiched between two dielectric substrates and the radiating patch is on top of the upper substrate. The advantages of this kind of feeding technique are elimination of spurious feed radiation and high bandwidth due to overall increase in the thickness of the microstrip patch antenna. Impedance matching is achieved by controlling the length of the feed line and the width-to-line ratio of the patch [5].
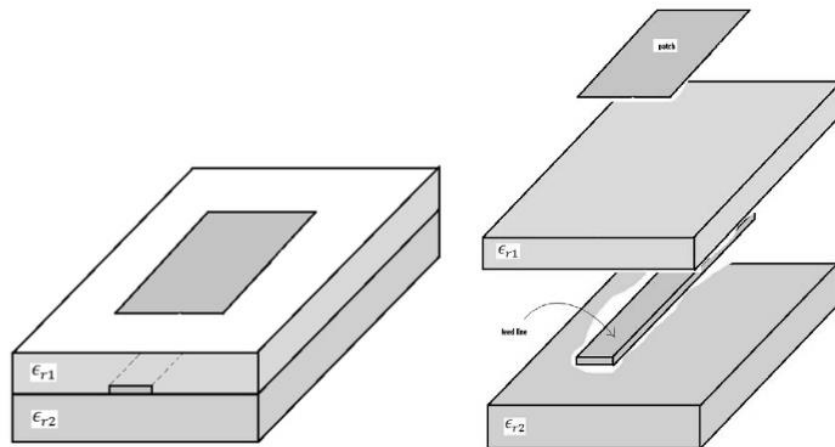
Figure 1.5 Proximity Coupled Feed

1.4 Comparison Microstrip Antenna Feeding Techniques

The Following table shows the comparison between all feeding techniques used in microstrip patch antennas.

Table 1.1 Comparison of the Characteristics of different Feeding Technics.

Characteristics / Techniques	Spurious feed Radiation	Reliability	Impedance Matching	Bandwidth (%)
Microstrip Line Feed	More	Better	Easy	2-5
Coaxial Feed	More	Poor	Easy	2-5
Aperture Coupled Feed	More	Good	Easy	13
Proximity Coupling Feed	Less	Good	Easy	21

1.5 Selection of Proximity Coupled Feeding Technique

Reasons for the selection of the Proximity Coupling Feed over the other feeding technics.

- Higher Bandwidth
- Highly reliable feeding technique
- Impedance matching is easy
- Has less spurious radiations
- No direct contact between feed line and radiating patch

2. ANTENNA PARAMETERS

2.1 Radiation Pattern

The radiation pattern is a graphical depiction of the relative field strength transmitted from or received by the antenna [5]. Antenna radiation patterns are taken at one frequency, one polarization, and one plane cut. The patterns are usually presented in polar form with a dB magnitude scale. Since a Microstrip patch antenna radiates normal to its patch surface, the elevation pattern for $\phi = 0$ and $\phi = 90$ degrees would be important.
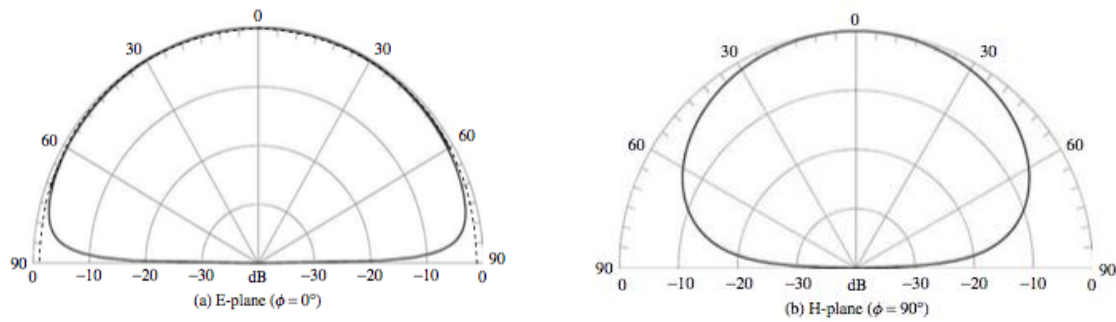
Figure 2.1 Radiation Pattern

2.2 Voltage Standing Wave Ratio (VSWR)

The most common case for measuring and examining VSWR is when installing and tuning transmitting antennas. When a transmitter is connected to an antenna by a feed line, the impedance of the antenna and feed line must match exactly for maximum energy transfer from the feed line to the antenna to be possible. When an antenna and feed line do not have matching impedances, some of the electrical energy cannot be transferred from the feed line to the antenna. Energy not transferred to the antenna is reflected back towards the transmitter. It is the interaction of these reflected waves with forward waves, which causes standing wave patterns. Matching the impedance of the antenna to the impedance of the feed line is typically done using an antenna tuner. The tuner can be installed between the transmitter and the feed line, or between

the feed line and the antenna. Both installation methods will allow the transmitter to operate at a low VSWR. Ideally, VSWR must lie in the range of 1-2.
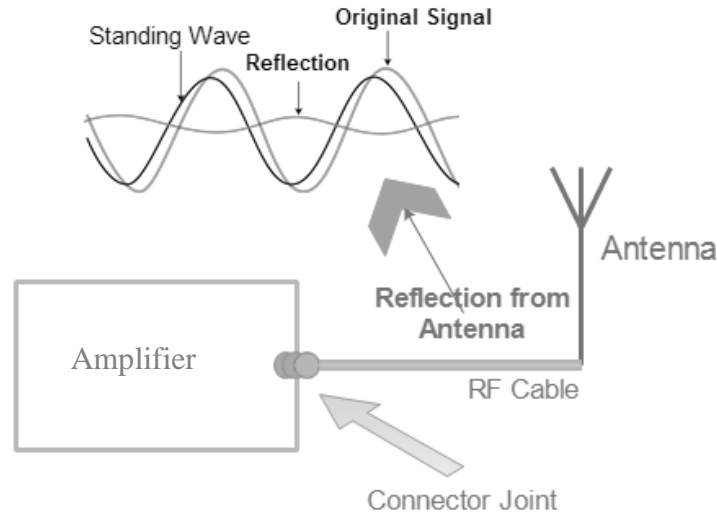
Figure 2.2 VSWR

2.3 Return Loss

The return loss (RL) is the parameter which indicates the amount of power that is lost to the load and does not return as a reflection (also known as S11). When the transmitter and the antenna impedance don't match the standing waves are formed because of the reflected waves [18]. The RL is the parameter similar to VSWR to indicate how well the matching between the transmitter and the antenna has taken place. The RL is defined as:

$$RL = -20 \, log10|\Gamma|, \tag{1}$$

In practical applications, the applicable VSWR of 1.5 or S11 of 0.2 is acceptable corresponds to an RL of -14 dB or 4% power reflection [5].

2.4 Gain

The gain of the antenna is closely related to the directivity, it is a measure that takes into account the efficiency of the antenna as well as its directional capabilities. Gain of an antenna (in a given

direction) is defined as "the ratio of the intensity, in a given direction, to the radiation intensity that would be obtained if the power accepted by the antenna were radiated isotropically [5].

$$Gain \; = \; \frac{4\pi * \; radiation \; intensity}{total \; input}$$

(2)

$$= \frac{4\pi \; U(\Theta, \varphi)}{P_{in}}$$

(3)

2.5   Directivity

Directivity of an antenna defined as the ratio of the radiation intensity in a given direction from the antenna to the radiation intensity averaged over all directions [5].

In mathematical form, it can be written as:

$$D \; = \frac{U}{U_o} \; = \; \frac{4\pi U}{Prad}$$

(4)

If the direction is not specified, it implies the direction of maximum radiation intensity. Directivity is dimensionless.

U= Radiation intensity (W/unit solid angle)

U_o= Radiation intensity of isotropic source (W/unit solid angle)

$Prad$ = Total radiated power (W)

2.6   Polarization

The polarization of an antenna is the polarization of the wave radiated from the antenna. A receiving antenna has to be in the same polarization as the transmitting antenna otherwise it will not resonate. Polarization is a property of the electromagnetic wave; it describes the magnitude and direction of the electric field vector as a function of time, with other words "the orientation of the electric field for a given position in space". A simple strait wire has one polarization when mounted vertically, and different polarization when mounted horizontally Figure 2.3.

Polarization can be classified as linear, circular, and elliptical. In linear polarization the antenna radiates power in the plane of propagation, only one plane, the antenna is vertically linear polarized when the electric field is perpendicular to the earth's surface, and horizontally linear polarized when the electric field is parallel to the earth's surface.

Figure 2.3 Polarization of electromagnetic wave

2.7   Transmission Line Model

This model is considered as the simplest and normally used in understanding the basic performance of the microstrip antenna. Originally this model was developed for rectangular patch but has been extended for generalized patch shapes. In this modeling the microstrip antenna is represented by two slots of width W and height h, separated by a transmission line with length L. The microstrip is a non-homogeneous line of two dielectrics, typically the substrate and air [17]. The width of the radiated patch is given by [5] as:

$$W = \left(\frac{3 * 10^8}{2 * f}\right) * sqrt\left(\frac{2}{\varepsilon_r + 1}\right) * 1000$$

(5)

(a) (b)

Figure 2.4 (a) Microstrip Line (b) Electric field Lines

Looking at the Figure 2.4 (a), most of the electric field lines reside in the substrate and parts of some lines are in the air. For that, this transmission line cannot support the pure transverse-electric-magnetic (TEM) mode of transmission due to the fact that the phase velocities would be different in the air and the substrate. Instead, the dominant mode of the propagation would be the quasi-TEM mode, means that the effective dielectric constant ε_{reff} must be obtained in order to account for the fringing and the wave propagation in the line.

The value of ε_{reff} is slightly smaller than ε_r since the fringing fields around the periphery of the patch are not confined in the dielectric substrate, but also spreading the as shown in Figure 2.4 (b). Based on Balanis [5], the expression for ε_{reff} is given by:

$$\varepsilon_{reff} = \left(\frac{\varepsilon_r + 1}{2}\right) + \left(\frac{\varepsilon_r - 1}{2}\right) * \left(1 + \left(\frac{12 * h}{W}\right)\right)^{-0.5}$$

(6)

Where

ε_{reff} = Effective dielectric constant

ε_r = Dielectric constant of substrate

h = Height of dielectric substrate

W = Width of the patch

The fringing fields along the width can be modeled as radiating slots and electrically the patch of the microstrip antenna looks greater than its physical dimensions. The dimension of the patch along its length have now been extended on each end by a distance ΔL, which is given empirically by [5] as,

$$\Delta L = \left(\frac{\left(\varepsilon_{reff} + 0.3\right) * \left(\left(\frac{W}{h}\right) + 0.264\right)}{\left(\varepsilon_{eff} - 0.258\right) * \left(\left(\frac{W}{h}\right) + 0.8\right)}\right) * (0.412 * h)$$

(7)

The effective length of the patch L_{eff} now becomes,

$$L_{eff} = L + 2\Delta L$$

(8)

For a given resonance frequency f_o, the effective length is given by [5] as:

$$L_{eff} = \left(\frac{3e8}{2 * f * sqrt(\varepsilon_{reff})}\right) * 1000$$

(9)

Therefore, the actual length is:

$$L = L_{eff} - 2\Delta L$$

(10)

The minimum ground plane length and width,

$$L_g = 6h + L$$

(11)

$$W_g = 6h + W$$

(12)

2.8   Impedance Matching

The theory of maximum power transfer states that for the transfer of maximum power from a source with fixed internal impedance to the load, the impedance of the load must be the same of the source. Most microwave applications are designed with an input impedance of 50Ω, so matching the antenna to 50Ω is our desire.

$$Z_S = Z_L^*$$

(13)

Z_S = Impedance of the source.

Z_L^*= Impedance of the load.

(*) indicates the complex conjugate.

We can begin with representing the patch by a parallel equivalent admittance Y as shown in Figure 2.5.
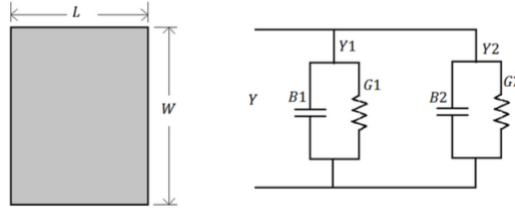
Figure 2.5 Rectangular Patch and its transmission model equivalent

Where:

$$Y = \frac{1}{Z_L} = G + jB$$

(14)

$$Y_1 = Y_2$$

(15)

$$G_1 = G_2$$

(16)

$$B_1 = B_2$$

(17)

A general expression for the conductance G_1 is given by [5, 17, and 23]

$$G_1 = \frac{2P_{rad}}{|V_0|^2}$$

(18)

Where:

P_{rad}= Radiation power

V_0= Voltage across the slot

$$P_{rad} = \frac{|V_0|^2}{2\pi\eta_0} \int_0^\pi \left[\frac{\sin\left(\frac{k_0 W}{2}\cos\theta\right)}{\cos\theta}\right]^2 \sin\theta^3 \, d\theta$$

(19)

$$G_1 = \frac{I_1}{120\pi^2}$$

(20)

Where

$$I_1 = \int_0^\pi \left[\frac{\sin\left(\frac{k_0 W}{2}\cos\theta\right)}{\cos\theta}\right]^2 \sin\theta^3 \, d\theta$$

(21)

$$I_1 = -2 + \cos(x) + \left(x * sinint(x)\right) + \left(\frac{\sin(x)}{x}\right)$$

(22)

$$x = K_o * W$$

(23)

$$K_o = \frac{2\pi}{l_a}$$

(24)

$$l_a = \left(\frac{3e8}{f}\right) * 1000$$

(25)

According to C. Balanis [18] taking into account the mutual effects of the parallel equivalent admittance Y_1 and Y_2 shown in Figure 2.5;

$$R_{in} = \frac{1}{2(G_1 \mp G_{12})}$$

(26)

Where "the (+) sign is used for modes with odd (antisymmetric) resonant voltage distribution beneath the patch and between the slots while the minus (-) sign is used for modes with even (symmetric) resonant voltage distribution" [18].

$$G_{12} = \frac{1}{|V_o|^2} \iint_S E_1 \times H_2^* \, ds$$

(27)

Where

E_1=Electric field radiated by Y_1

H_2^*=Magnetic field radiated by Y_2

J_0= Bessel function of the first kind of order zero.

$$G_{12} = \frac{1}{120\pi^2} \int_0^\pi \left[\frac{\sin\left(\frac{k_0 W}{2}\cos\theta\right)}{\cos\theta} \right]^2 * J_0(k_0 L \sin\theta) \sin\theta^3 \, d\theta$$

(28)

Finally, the position of feed point of the patch (where the impedance of the patch at that point is 50Ω) can be found from the following equation:

$$R_{in} = \frac{1}{2(G_1 \mp G_{12})} \cos\left(\frac{\pi}{L}y_o\right)^2$$

(29)

Therefore, the Inset feed point distance is:

$$y_0 = \left(\frac{L}{\pi}\right) * \left(acos\left(sqrt\left(\frac{Z_0}{R_{in}}\right)\right)\right)$$

(30)
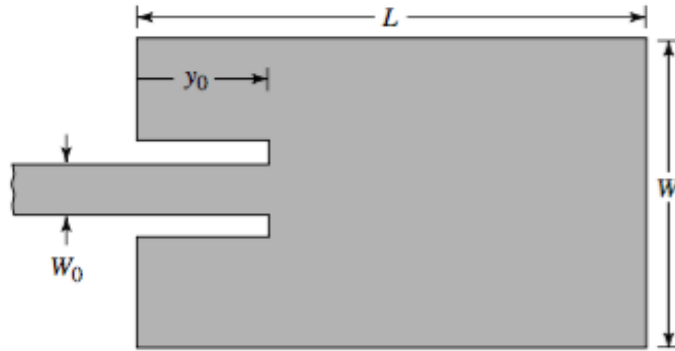
Figure 2.6 Inset feed point distance (y_0)

To match the patch antenna using a microstrip line feed whose characteristic impedance (Z_0) is 50 ohms a transmission line width (W_0) has to be calculated, given as:

$$W_0 = h * \left(\frac{2}{\pi}\right) * \left(B - 1 - m + \left(\left(\frac{\varepsilon_r - 1}{2 * \varepsilon_r}\right) * \left(n + 0.39 * \left(\frac{0.61}{\varepsilon_r}\right) \right) \right) \right)$$

(31)

Where,

$$B = \frac{377\pi}{2 * Z_o * \sqrt{\varepsilon_r}}$$

(32)

$$m = \log(2 * B - 1)$$

(33)

$$n = \log(B - 1)$$

(34)

3. OCTAGONAL PATCH DESIGN

3.1 Octagonal Patch Antenna using Proximity Feeding Technique

This configuration uses two-layer substrate with the microstrip line on the lower layer and the octagonal patch antenna on the upper layer. The feed line terminates in an open and underneath the patch. This feed is better known as an "electromagnetically coupled" microstrip feed. Coupling between the patch and the microstrip is capacitive in nature [16]. The substrate parameters of two layers can be selected to increase the bandwidth of the patch and to reduce the spurious radiations from the open end of the microstrip. The radiating patch being placed on the double layer gives a larger bandwidth.
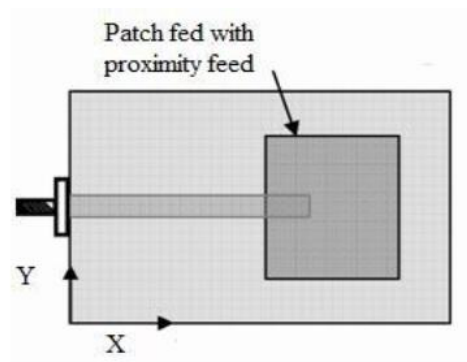
Figure 3.1 Geometry of a Proximity Coupled Microstrip Feed Patch Antenna
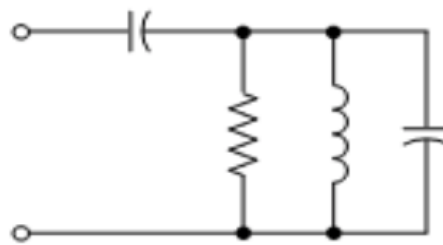
Figure 3.2 Equivalent Circuit of Proximity Coupled Feed

3.2   The design of the patch antenna parameters

1) The dielectric constant of the substrate (ε_r)
2) The resonant frequency (f_r)
3) The height of the substrate (h)

3.2.1   Dielectric Constant of the Substrate (ε_r)

The dielectric constant of substrate material plays an important role in the patch antenna design. A substrate with a high dielectric constant reduces the dimensions of the antenna but it also affects the antenna performance. So, there is a trade-off between size and performance of patch antenna.

3.2.2   Frequency of Operation (f_r)

The resonant frequency of the antenna must be selected appropriately. The Mobile Communication Systems uses the frequency range from 900-5800 MHz's Hence the antenna designed for the mobile communication system must be able to operate in this frequency range. The resonant frequency selected for my design is 900 MHz, 1.8 GHz and 2.4 GHz.

3.2.3   Height of Dielectric Substrate (h)

For the Microstrip patch antenna to be used in communication systems, it is essential that the antenna is not bulky. Hence, the height of the dielectric substrate should be less.

3.1   Design Procedure of Dual Band Octagonal Patch Antenna

After the proper selection of above three parameters, the next step is to calculate the radiating patch width and length. By using all these given parameters, the length and width of patch is calculated using the microstrip antenna patch calculator.

Step 1: Calculation of Width (W)

For an efficient radiator, practical width that leads to good radiation efficiencies is calculated by transmission line model equation (5) .

Step 2: Calculation of Effective Dielectric Coefficient (ε_{reff})

The effective dielectric constant is obtained by referring to equation (6).

Step 3: Calculation of Effective Length (L_{eff})

The effective length is calculated using equation (9).

Step 4: Calculation of Length Extension (ΔL)

The value of ΔL can be obtained by using equation (7).

Step 5: Calculation of Actual Length of Patch (L)

The actual length of radiating patch is calculated using equation (10).

Step 6: Calculation of Ground Dimensions (L_g, W_g)

The transmission line model is applicable to infinite ground planes only. However, for practical considerations, it is essential to have a finite ground plane. It has been shown by that similar results for finite and infinite ground plane can be obtained if the size of the ground plane is greater than the patch dimensions by approximately six times the substrate thickness all around the periphery. The minimum length and width of the ground plane is calculated using equations (11) and (12).

Step 7: Calculation of the Conductance of the Patch (G_1)

The length of the feed is calculated using equation (20).

Step 8: Calculation of the Mutual Conductance of the Patch (G_{12})

The length of the feed is calculated using equation (27).

Step 9: Calculation of the Input Impedance of the Patch (R_{in})

The length of the feed is calculated using equation (26).

Step 10: Calculation of the Length of the Feed Line (y_0).

The length of the feed is calculated using equation (30).

Step 11: Calculation of the Width of the Feed Line (W_0).

The width of the feed is calculated using equation (31)

3.2   Design of Dual Band Octagonal Microstrip Patch Antenna Using Proximity Coupling Feed for 900 MHz and 1.8 GHz.

The dual band octagonal microstrip patch antenna (OMPA) resonating at 900 MHz and 1.8 GHz for Energy Harvesting applications can be designed using the following specifications:

Table 3.1 Dual Band Octagonal Microstrip Patch Antenna Specifications

Variable	Value
Dielectric Constant	9.8
Resonant Frequency	0.9-1.8 GHz
Height of the substrate	1.6 mm

3.2.1   Antenna Design

The radiating octagonal patch is printed on the upper side of the first substrate. The dimensions of the octagonal patch are stated in Table 3.2 calculated using transmission line equation referring to section 2.7 topics. The two substrates used are of same material and have same height. The substrate is made up of Ceramic material having dielectric constant of 9.8 and height of the substrate is 1.6 mm. The proximity coupling feed line is between the two substrates. The width of the feed line and the length from the center of the microstrip towards the patch axis along the positive y direction are stated in Table 3.2.

The following parameters for antenna design are calculated by using the above steps of the antenna design using the transmission line model equations.

Table 3.2 Dimensions of the OMPA

Variable	Value
Width of Patch one (W_{p1})	71 mm
Length of Patch one (L_{p1})	53 mm
Width of patch two (W_{p2})	35 mm
Length of Patch two (L_{p2})	26 mm
Width of the Ground Plane (W_g)	81 mm
Length of the Ground Plane (L_g)	62 mm
Width of the feed (W_0)	1.3 mm
Length of the feed (y_0)	10 mm
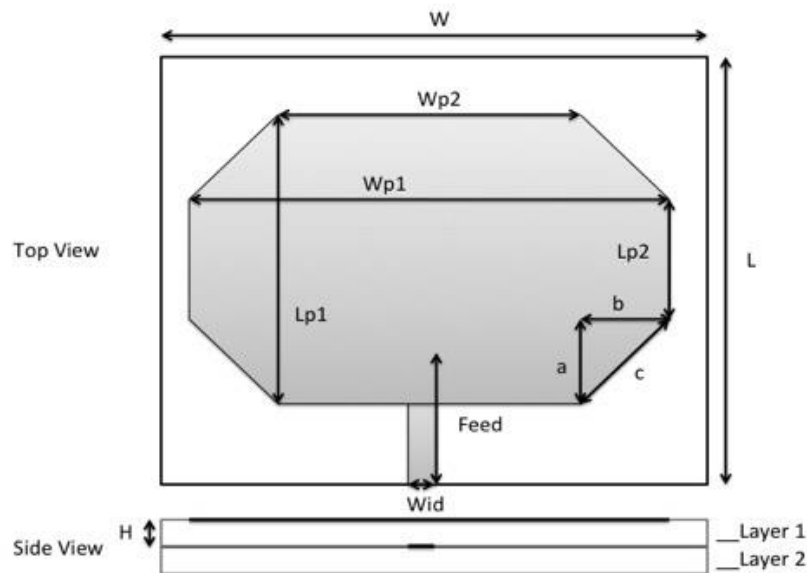
Figure 3.3 OMPA Dimensions Layout

3.3 Simulation Results

Figure 3.4 show the results obtained from the calculated dimensions for the octagonal patch antenna. The marker m1 show 940 MHz @ -6.6357 dB and m2 show 1.82 GHz @ -6.9307. To improve the performance of the octagonal microstrip antenna three optimizations steps are needed.
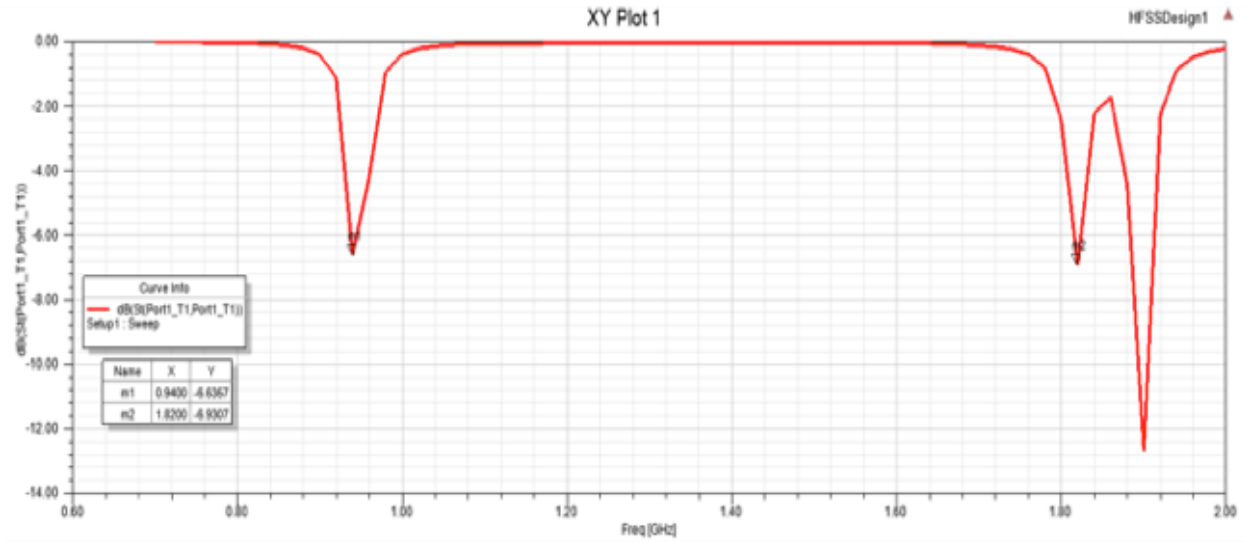
Figure 3.4 Simulation of return loss without any optimization.

3.3.1 Optimization Parametric of the Antenna

In this section, three optimizations parameters like width of the feed line, length of the feed line and width of the patch are studied, by varying one parameter at a time and keeping all others parameters constant.

3.3.1.1 Effect of Feed Length

The Figure 3.5 shows the effect of the proximity coupling feed length on the return loss. By increasing the length of the feed the return loss of the lower frequency decrease. The optimize value for the length of the feed is 16 mm.
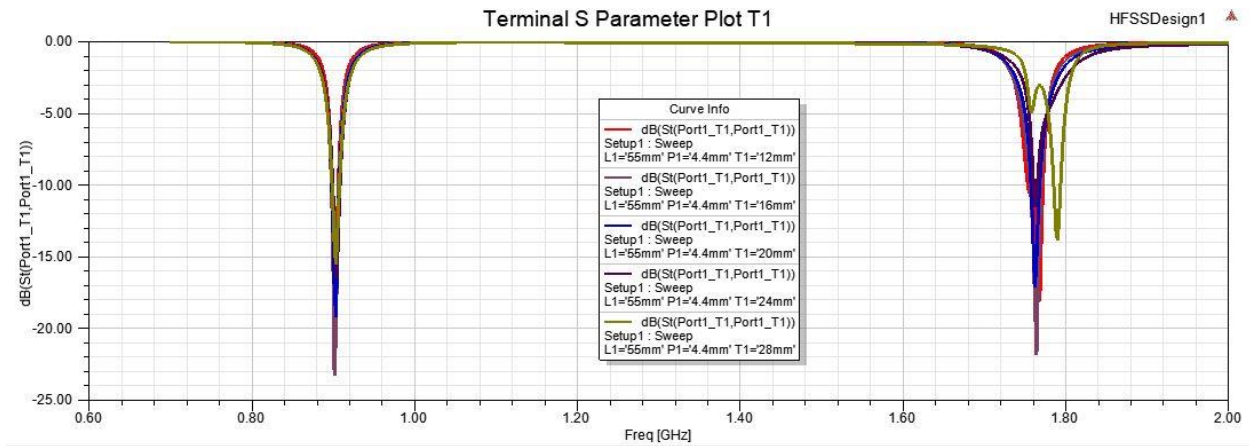
Figure 3.5 Variation of S parameter with respect to the length of the feed line.

3.3.1.2 Effect of the Feed Width

The Figure 3.6 shows the effect of the proximity coupling feed width on the return loss. By increasing the width of the feed the return loss of the higher frequency decrease. The optimize value for the width of the feed is 4.4 mm.
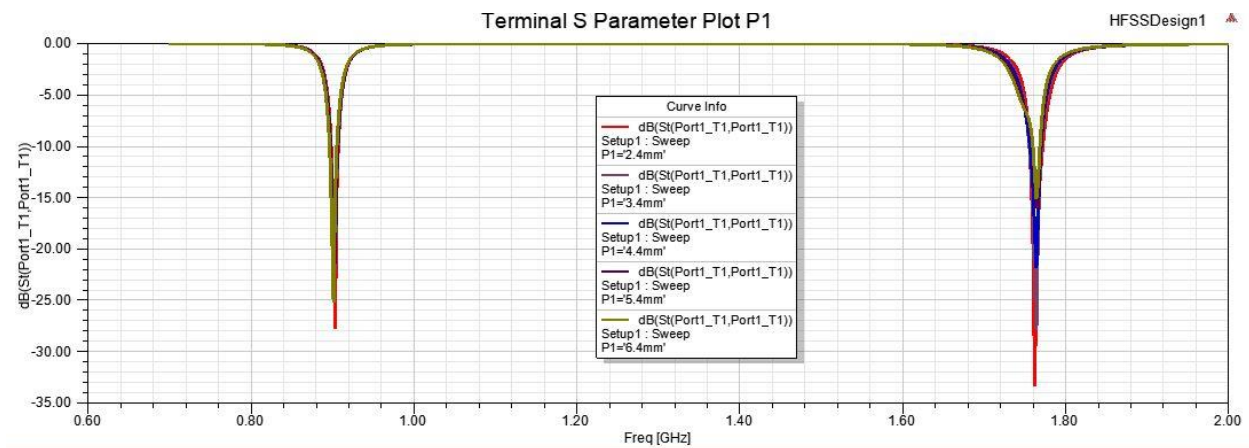
Figure 3.6 Variation of S parameter with respect to the width of the feed line.

3.3.1.3 Effect of the Patch Width

The Figure 3.7 shows the effect of the width of the Patch on the return loss. Increasing or decreasing the width of the patch can tune the frequencies. The optimize value for the width of the patch is 55 mm.
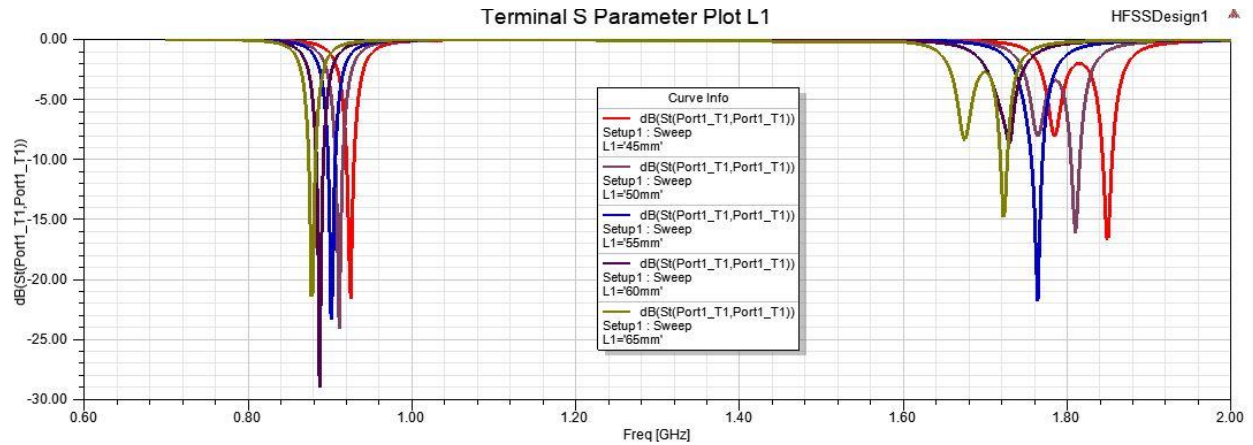
Figure 3.7 Variation of S parameter with respect to the width of the patch.

3.3.1.4 Optimized Dimensions

The Figure 3.8 shows the optimized values for the octagonal microstrip patch antenna at 900 MHz and 1.8 GHz.
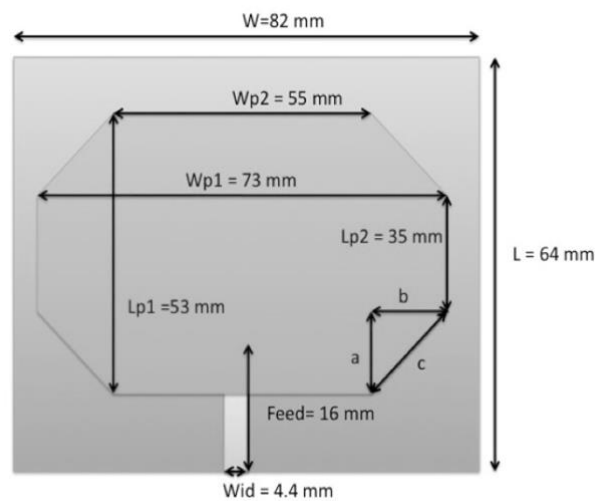
Figure 3.8 Optimized Dimension Layout of the OMPA

3.3.2 Final Simulation Results

The simulated antenna design using High Frequency Simulation Structure (HFSS) is given in Figure 3.9.

Figure 3.9 Designed Structure of OMPA on HFSS

The simulation results of the designed antenna of various parameters like return loss, impedance, gain, VSWR and directivity are given using HFSS.
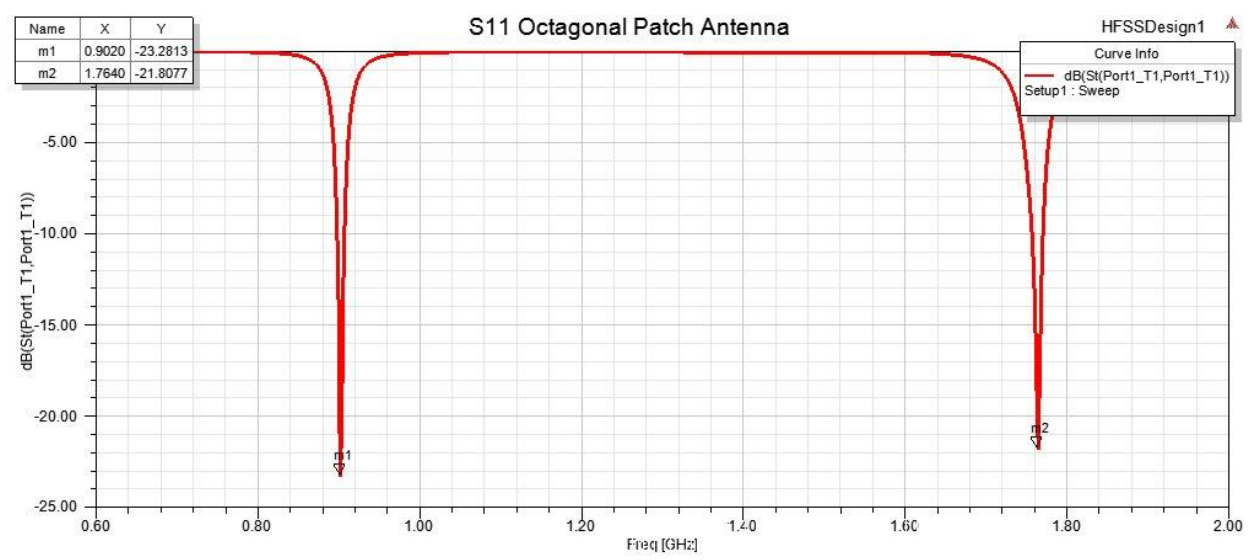
Figure 3.10 Simulated Return Loss of OMPA

The above designed antenna shows good return loss approximately -21.5 dB at 900 MHz and - 20.3 dB at 1.8 GHz, which is an excellent result. This antenna resonates at frequencies, which is applicable for GSM and WIFI technologies.

The proposed antenna design gives good impedance of approximately 50.7 ohms at 900 MHz and 50.7 at 1.8 GHz, which shows that the antenna is perfectly matched, and the power loss is minimum. The result of the designed antenna is given below in Figure 3.11:
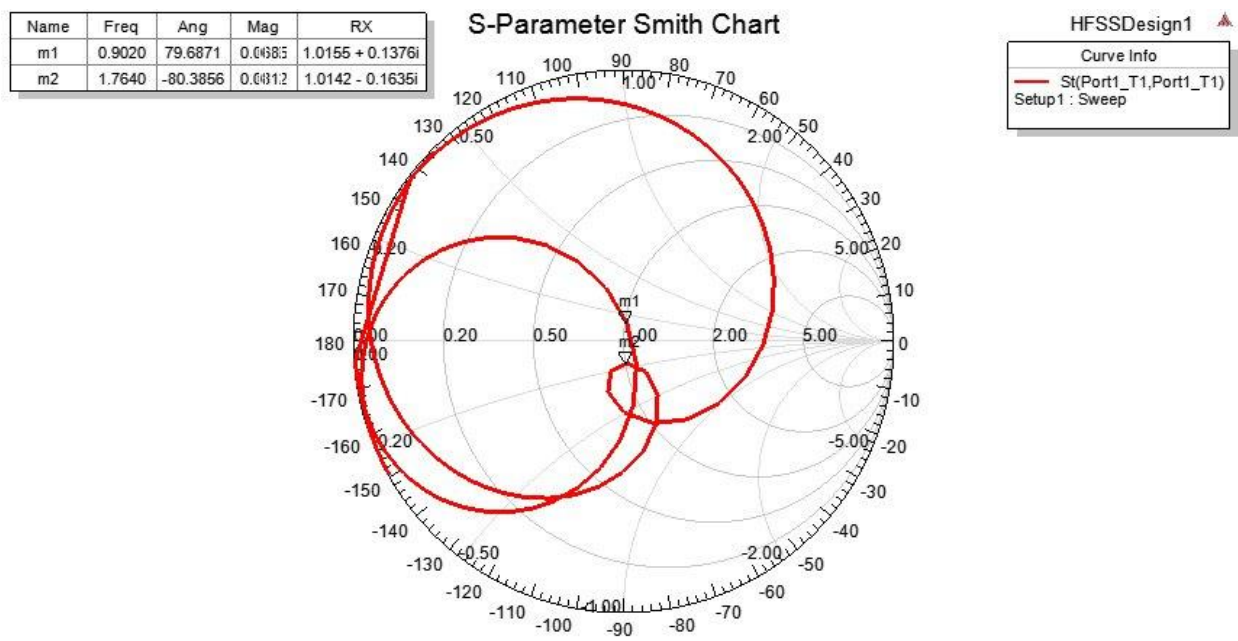
Figure 3.11 Smith Chart of OMPA

In the following Figure 3.12 shows the VSWR of 1.18 at 900 MHz and 1.21 at 1.8 GHz. Which means that a good impedance match has been made and a very small amount of the source wave will be lost.

Figure 3.12 Simulated VSWR of OMPA

The simulation Results of Radiation Pattern of Phi at $0°$ and $90°$ for 900 MHZ and 1.8 GHz are given below:

Figure 3.13 Simulated Radiation Pattern Phi= $0°$

Figure 3.14 Simulated Radiation Pattern Phi= 90°

The Figure 3.13 and Figure 3.14 show the radiation pattern (RP) of the optimized antenna. The red line is the RP for 900 MHz and the violet line for 1.8 GHz. The readings are capture at a constant Phi and theta is the sweep from 0° to 180°.

The simulation of the gain of the optimized antenna is given in Figure 3.15.

Figure 3.15 Simulated OMPA Total Gain

The results of the above designed OMPA are summarized in the following table.

Table 3.3 Summary of Parameter Values of Designed OMPA

Parameters	Values	
Operating Frequencies	0.9 GHz	1.8 GHz
Return Loss	-21.5 dB	-20.3
Impedance	50.7 Ω	50.7 Ω
VSWR	1.18	1.21
Gain	-1.38 dB	-1.42 dB

3.4   Design of Dual Band Octagonal Microstrip Patch Antenna Using Proximity Coupling Feed for 900 MHz and 2.4 GHz.

The dual band octagonal microstrip patch antenna (OMPA) resonating at 900 MHz and 2.4 GHz for Energy Harvesting applications can be designed using the following specifications:

Table 3.4 Dual Band Octagonal Microstrip Patch Antenna Specifications

Variable	Value
Dielectric Constant	9.8
Resonant Frequency	0.9-2.4 GHz
Height of the substrate	1.6 mm

3.4.1   Antenna Design

The radiating octagonal patch is printed on the upper side of the first substrate. The dimensions of the octagonal patch are stated in Table 3.5 calculated using transmission line equation referring to section 2.7 topics. The two substrates used are of same material and have same height. The substrate is made up of Ceramic material having dielectric constant of 9.8 and height of the substrate is 1.6 mm. The proximity coupling feed line is between the two substrates. The width of the feed line and the length from the center of the microstrip towards the patch axis along the positive y direction are stated in Table 3.5.

The following parameters for antenna design are calculated by using the above steps of the antenna design using the transmission line model equations.

Table 3.5 Dimensions of the OMPA

| Variable	Value
Width of Patch one	71mm
Length of Patch one	53 mm
Width of patch two	26 mm
Length of Patch two	19 mm
Width of the Ground Plane	81 mm
Length of the Ground Plane	62 mm
Width of the feed	1.3 mm
Length of the feed	16 mm
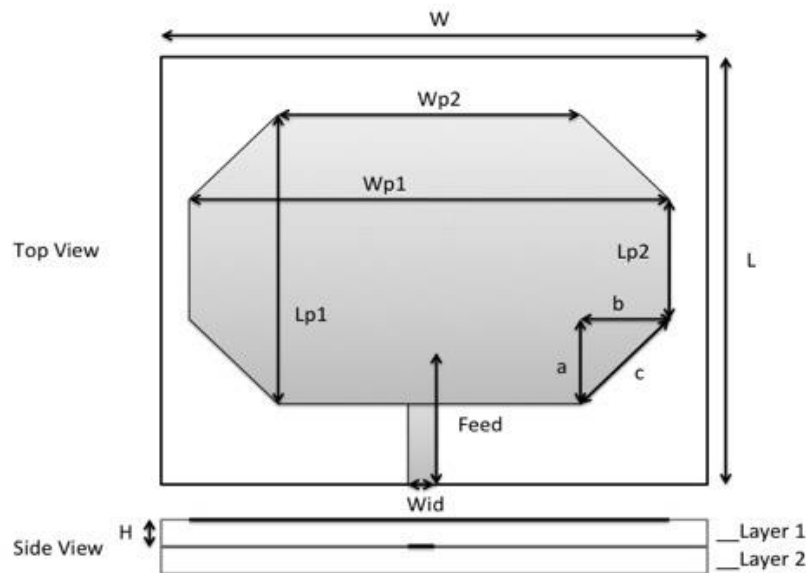
Figure 3.16 OMPA Dimensions Layout

3.5   Simulation Results

Figure 3.17 show the results obtained from the calculated dimensions for the octagonal patch antenna. . The marker m1 show 960 MHz @ -14.3314 dB and m2 show 2.52 GHz @ -5.6065 dB. To improve the performance of the octagonal microstrip antenna three optimizations steps are needed.
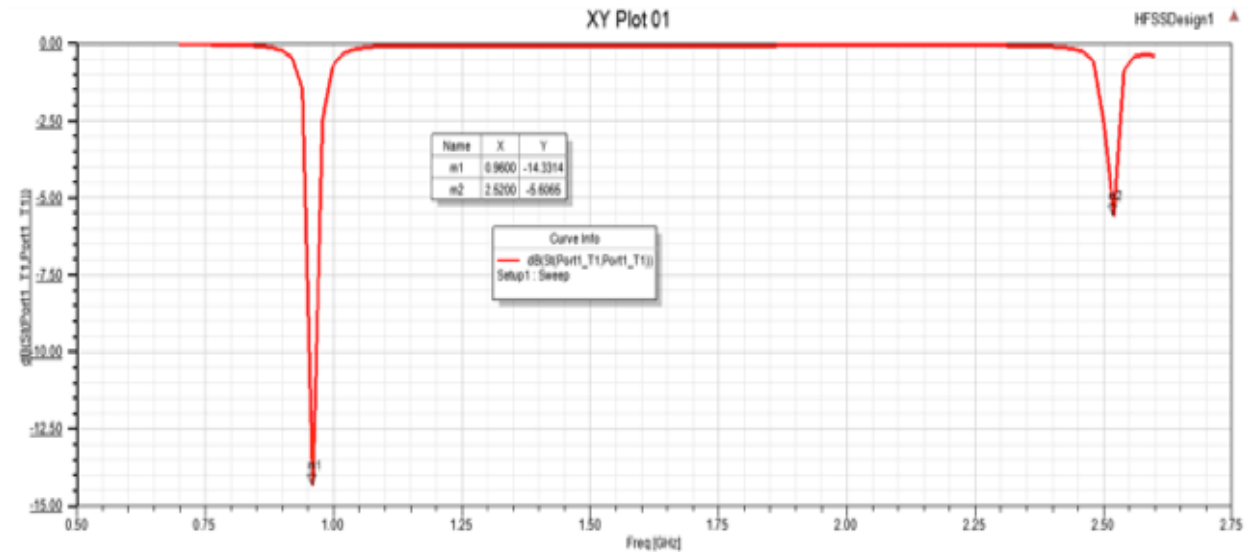
Figure 3.17 Simulation of return loss without any optimization.

3.5.1 Optimization Parametric of the Antenna

In this section, three optimizations parameters like width of the feed line, length of the feed line and width of the patch are studied, by varying one parameter at a time and keeping all others parameters constant.

3.5.1.1 Effect of Feed Length

The Figure 3.18 shows the effect of the proximity coupling feed length on the return loss. By increasing the length of the feed the return loss of the lower frequency decrease. The optimize value for the length of the feed is 22 mm.
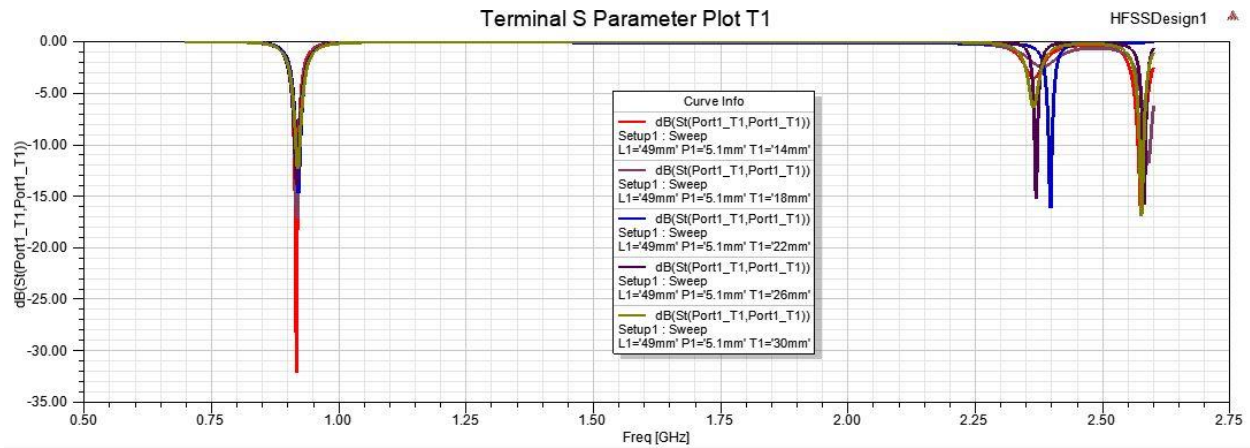
Figure 3.18 Variation of S parameter with respect to the length of the feed line.

3.5.1.2 Effect of the Feed Width

The Figure 3.19 shows the effect of the proximity coupling feed width on the return loss. By increasing the width of the feed the return loss of the higher frequency decrease. The optimize value for the width of the feed is 5.1 mm.
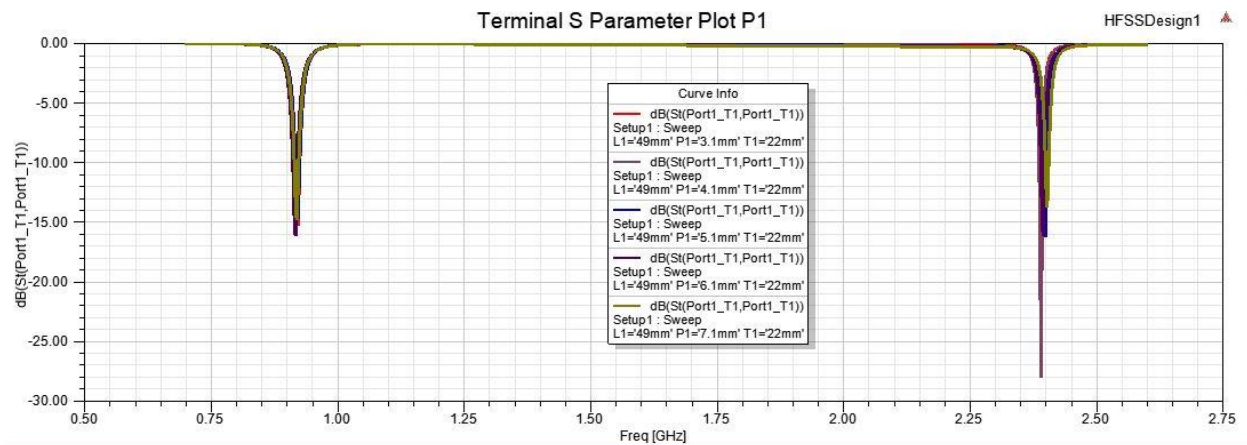
Figure 3.19 Variation of S parameter with respect to the width of the feed line.

3.5.1.3 Effect of the Patch Width

The Figure 3.20 shows the effect of the width of the Patch on the return loss. Increasing or decreasing the width of the patch can tune the frequencies. The optimize value for the width of the patch is 49 mm.
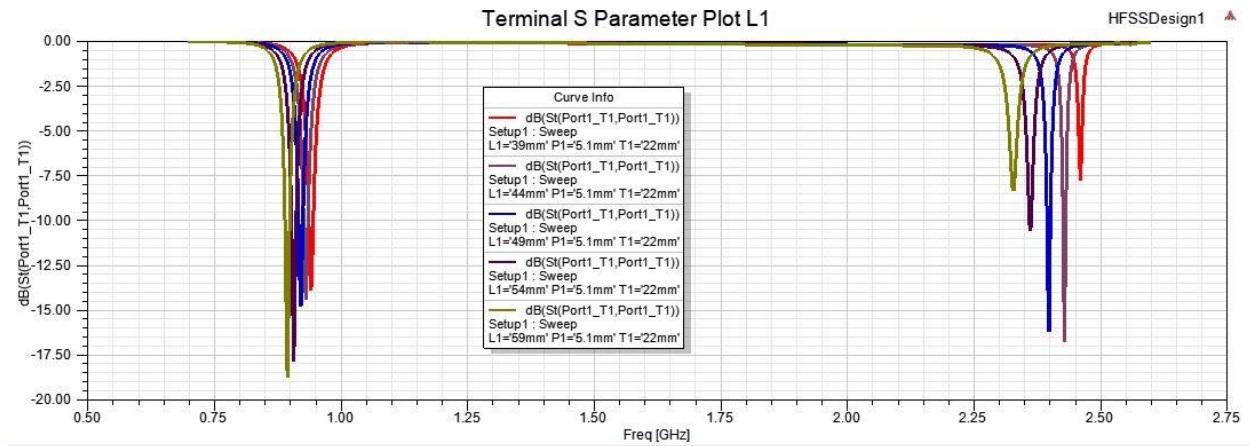
Figure 3.20 Variation of S parameter with respect to the width of the patch.

3.5.1.4 Optimized Dimensions

The Figure 3.21 shows the optimized values for the octagonal microstrip patch antenna at 900 MHz and 1.8 GHz.
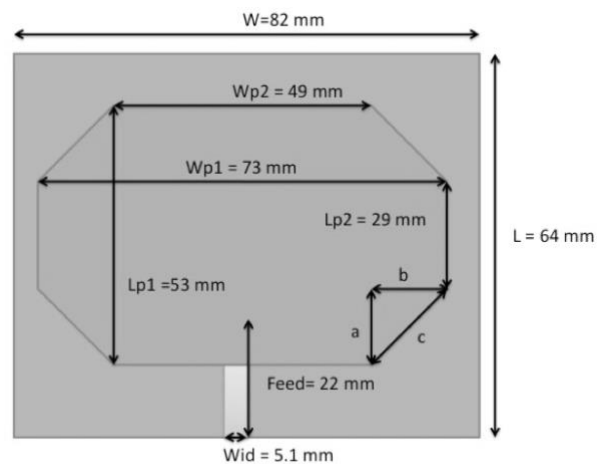
Figure 3.21 Optimized Dimension Layout of the OMPA

3.5.2 Final Simulation Results

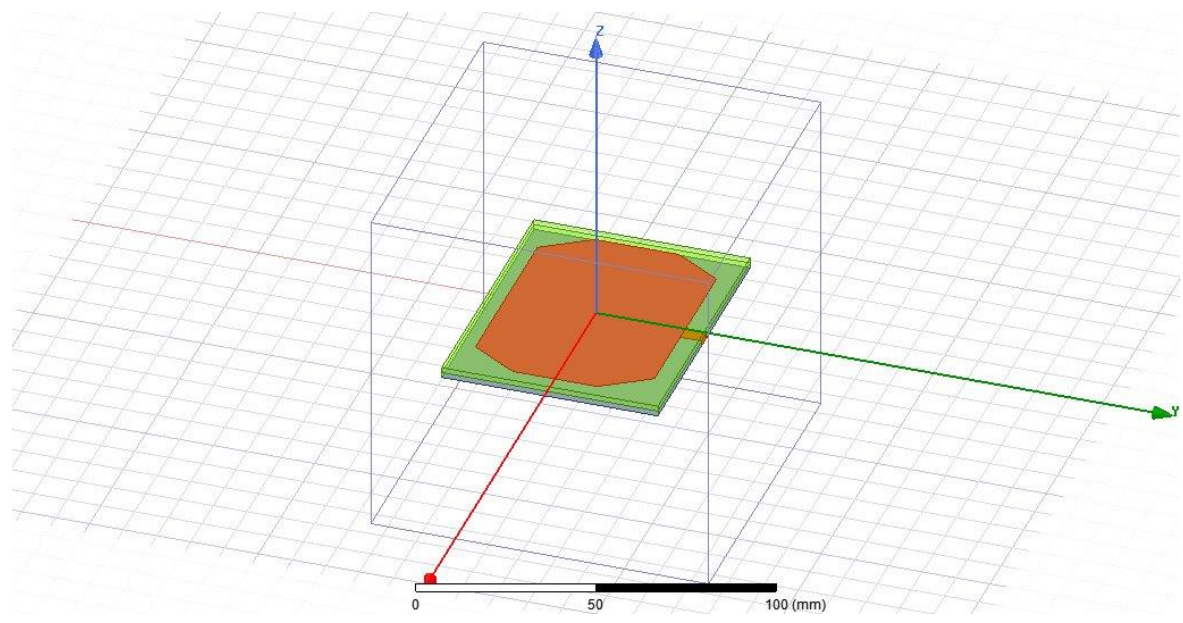The simulated antenna design using High Frequency Simulation Structure (HFSS) is given in Figure 3.22.
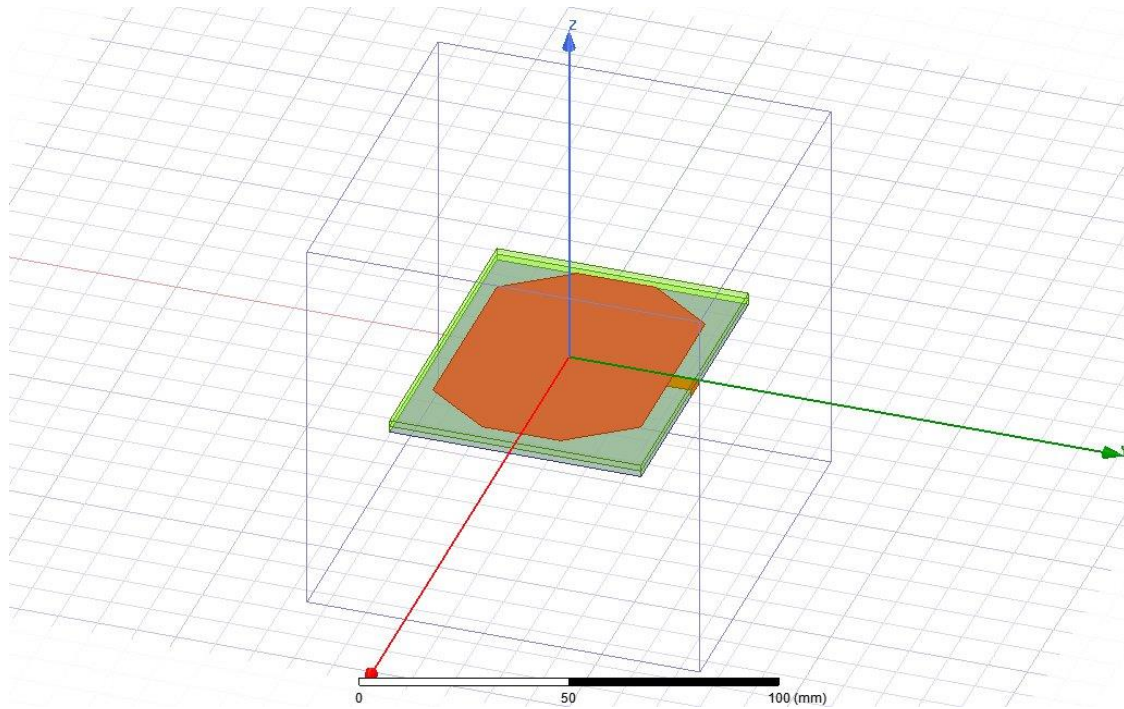
Figure 3.22 Designed Structure of OMPA on HFSS

The simulation results of the designed antenna of various parameters like return loss, impedance, gain, VSWR and directivity are given using HFSS.
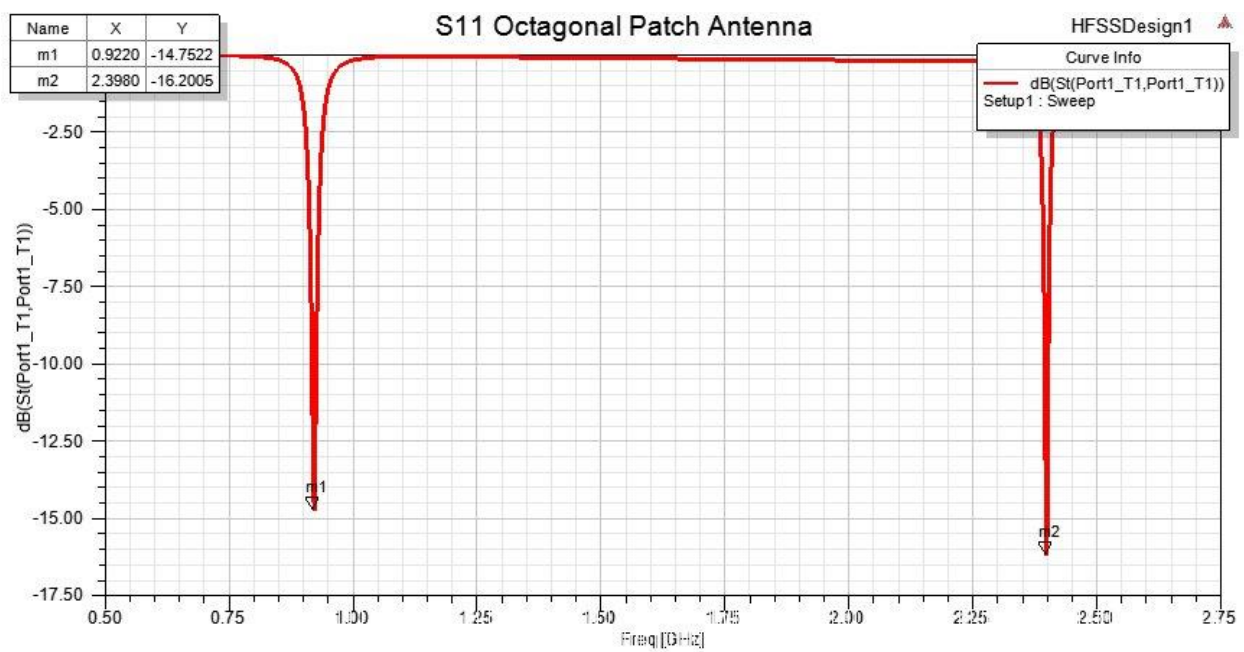
Figure 3.23 Simulated Return Loss of OMPA

The above designed antenna shows good return loss approximately -14.7 dB at 900 MHz and -16.3 dB at 1.8 GHz, which is an excellent result. This antenna resonates at frequencies that are applicable for GSM and WIFI technologies.

The proposed antenna design gives good impedance of approximately 71.3 ohms at 900 MHz and 50.6 at 1.8 GHz, which shows that the antenna is perfectly matched, and the power loss is minimum. The result of the designed antenna is given below in Figure 3.24:

Name	Freq	Ang	Mag	RX
m1	2.3980	78.6155	0.1549	1.0137 + 0.3154i
m2	0.9220	-13.3013	0.1830	1.4269 - 0.1243i
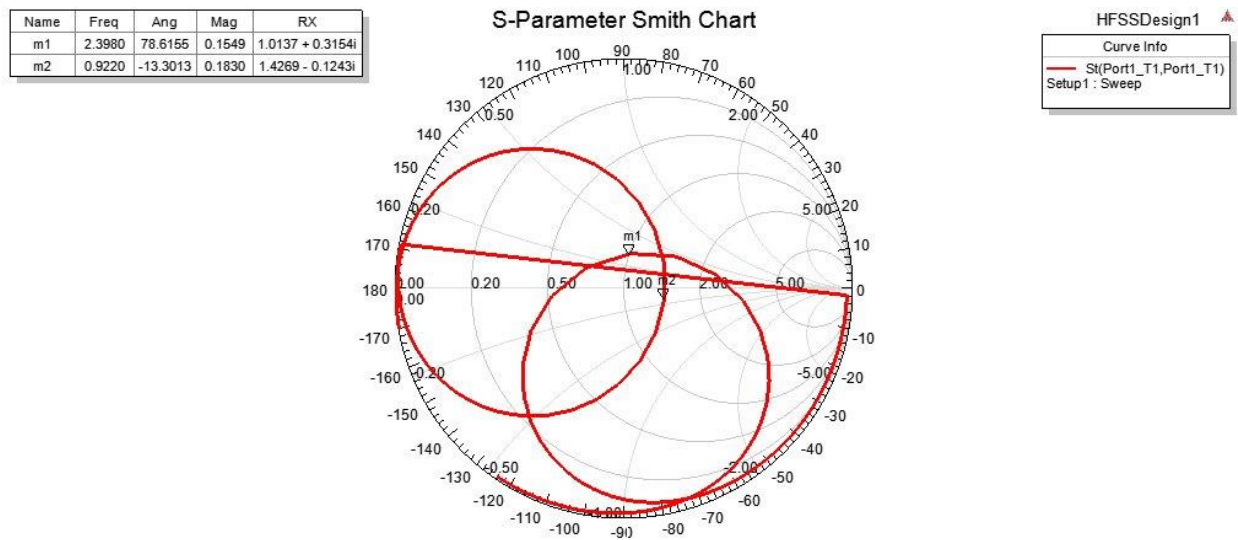
Figure 3.24 Smith Chart of OMPA

In the following Figure 3.25 shows the VSWR of 1.57 at 900 MHz and 1.65 at 1.8 GHz. Which means that a good impedance match has been made and a very small amount of the source wave will be lost.
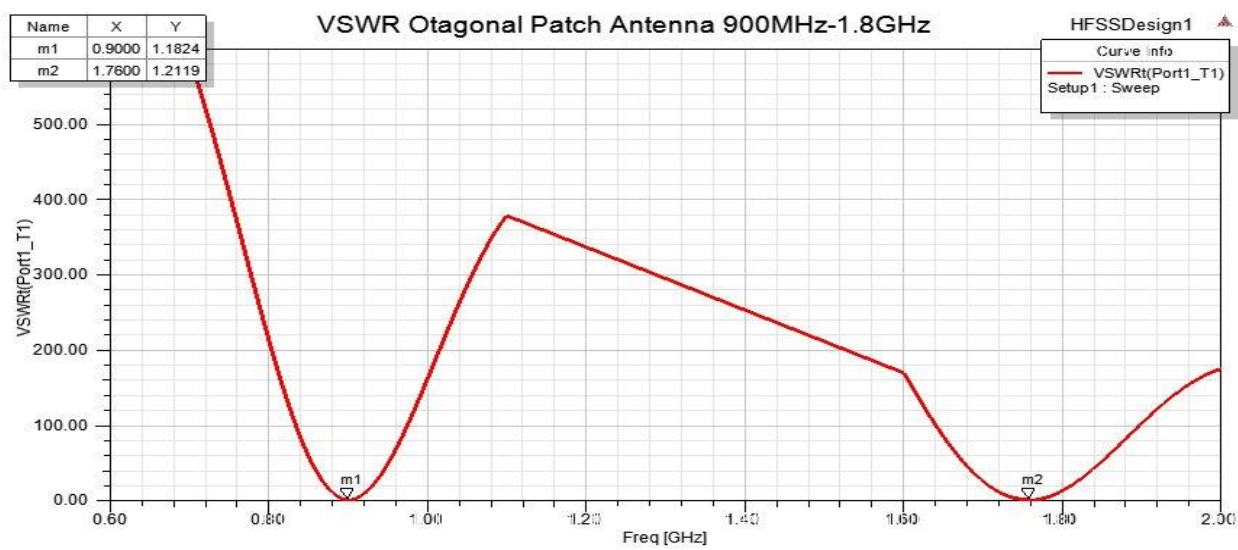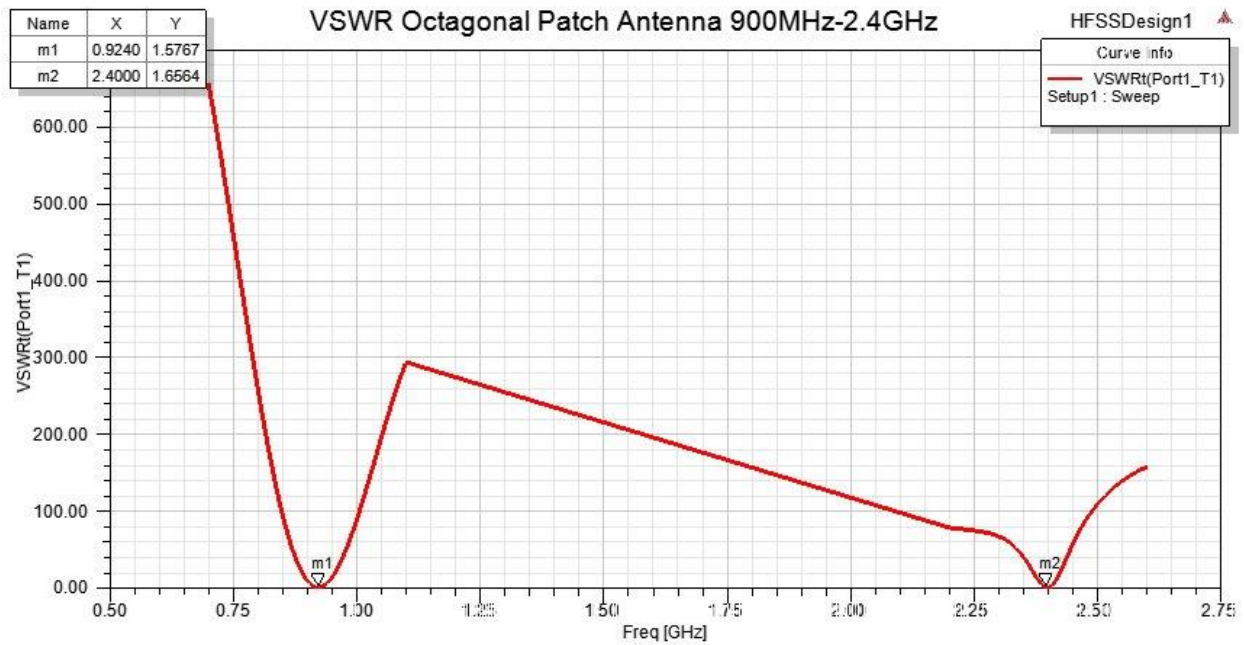
Figure 3.25 Simulated VSWR of OMPA

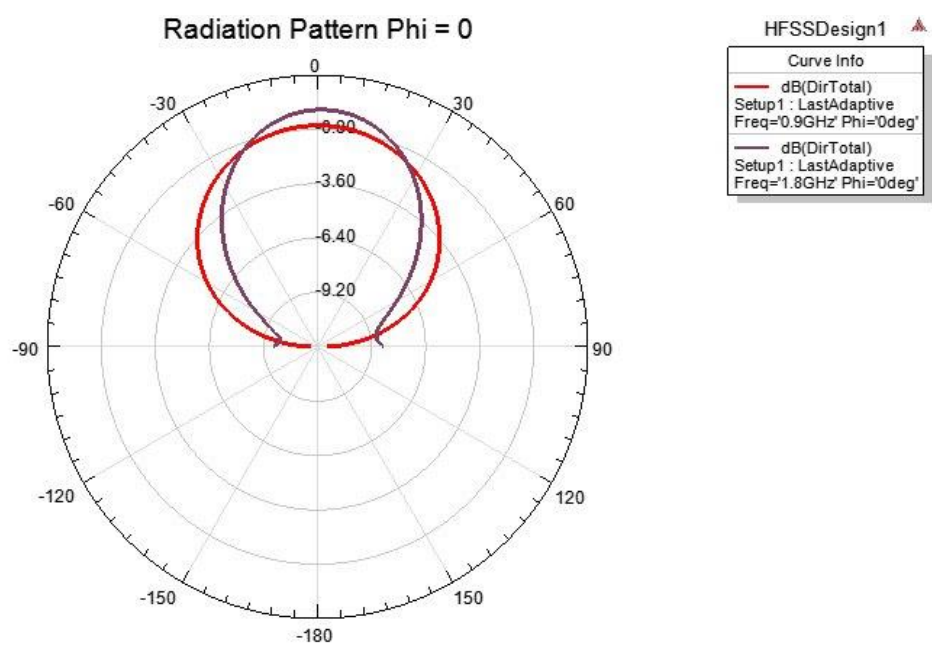The simulation Results of the Radiation Pattern of Phi at $0°$ and $90°$ for 900 MHZ and 2.4 GHz are given below
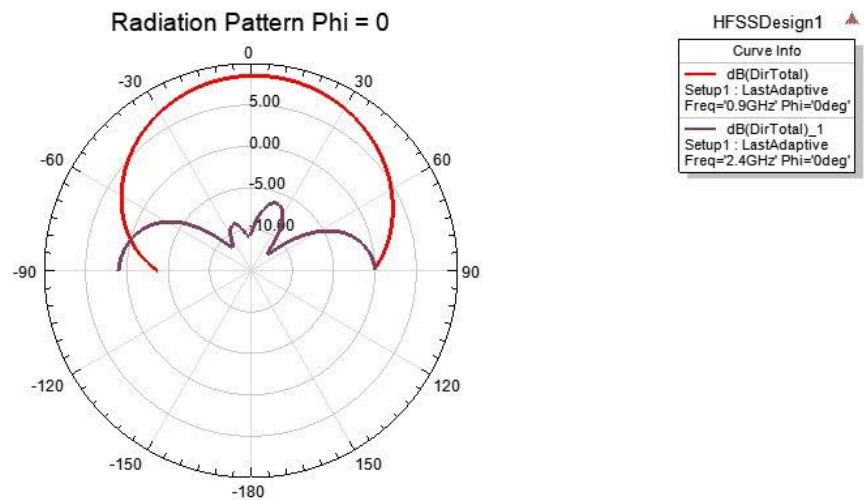
Figure 3.26 Simulated Radiation Pattern Phi= $0°$
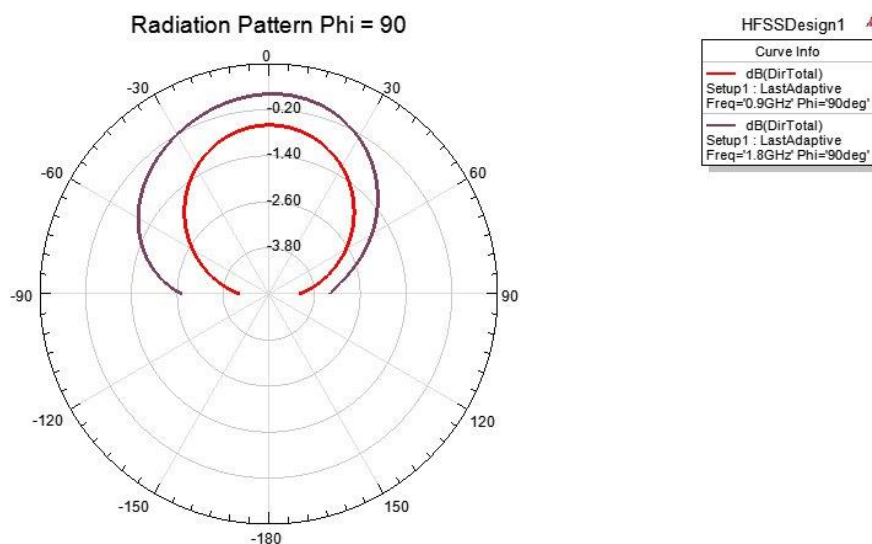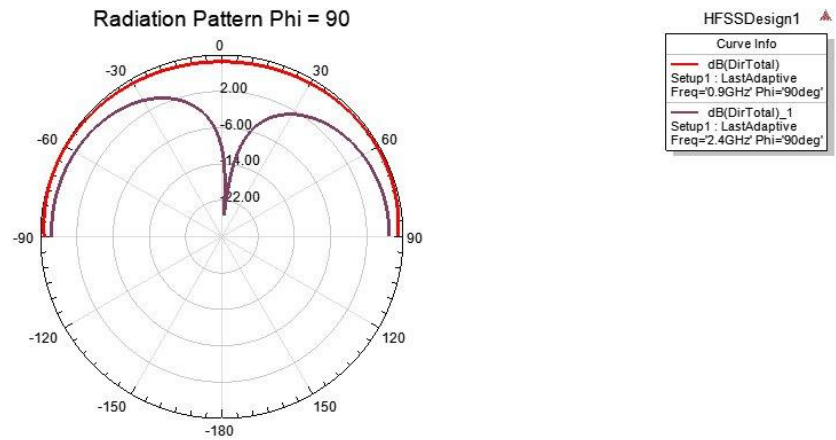
Figure 3.27 Simulated Radiation Pattern Phi= 90°

The Figure 3.26 and Figure 3.27 show the radiation pattern (RP) of the optimized antenna. The red line is the RP for 900 MHz and the violet line for 2.4 GHz. The readings are capture at a constant Phi and theta is the sweep from 0°to 180°.

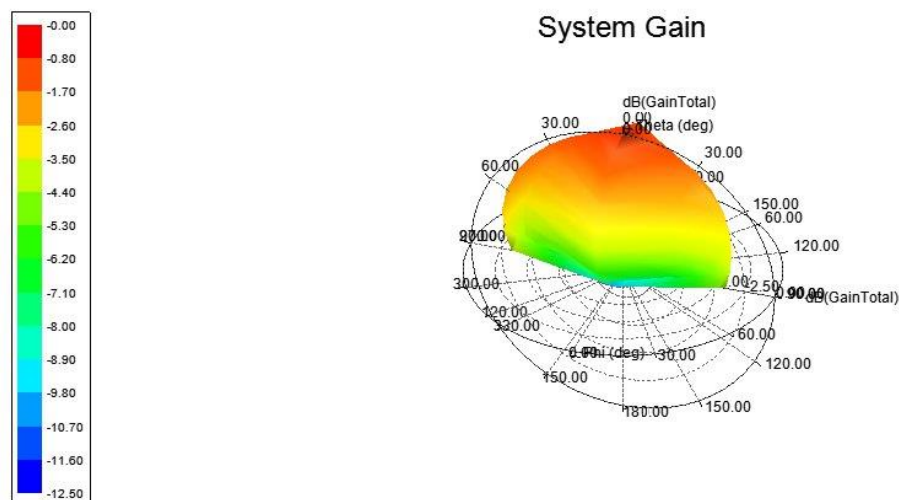The simulation of the gain of the optimized antenna is given in Figure 3.15.
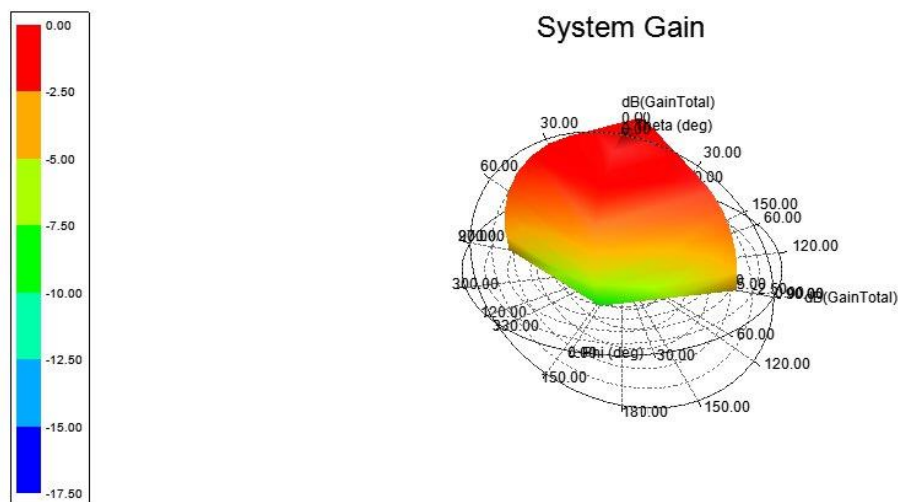
Figure 3.28 Simulated OMPA Total Gain

The results of the above designed OMPA are summarized in the following table.

Table 3.6 Summary of Parameter Values of Designed OMPA

Parameters	Values	
Operating Frequencies	0.9 GHz	2.4 GHz
Return Loss	-14.7 dB	-16.3 dB
Impedance	71.3 Ω	50.6 Ω
VSWR	1.57	1.65
Gain	4.98 dB	2.68 dB

4. FABRICATION OF ANTENNAS

4.1 Flow Chart of antenna Fabrication Process

Stage	Description
Design of the Gerber File	• The digital layout of top and bottom substrates layers were designed in DipTrace Software.
Copper removal of the substrate layers.	• The top and bottom layer were etch using the LPKF ProtoMat S103 circuit board plotter.
Bottom Copper Ground Layer	• A copper adhesive sheet was applied at the bottom of the lower substrate layer.
SMA Connector	• A SMA connector were soldered to the feed line (+) and the reference (-) to the ground plane layer.
Adhere Layers	• Both layers were adhere using 3M dual side micro dots glue.
Done	• Dual Band Octagonal Microstrip Patch Antenna is build.

Figure 4.1 Flow Chart of Antenna Fabrication Process

4.2 Equipment and Tools used for Fabrication Process

4.2.1 Dip Trace Schematic & PCB Design Software

Dip Trace Software is a high-level engineering tool for board design and wide import/export capabilities. The Following Figure 4.2 (a) shows the screen capture of the software with the bottom later design and Figure 4.2 (b) shows the screen capture of the Top Layer. After each layer was design it was exported as a Gerber file compatible with the cutting machine.
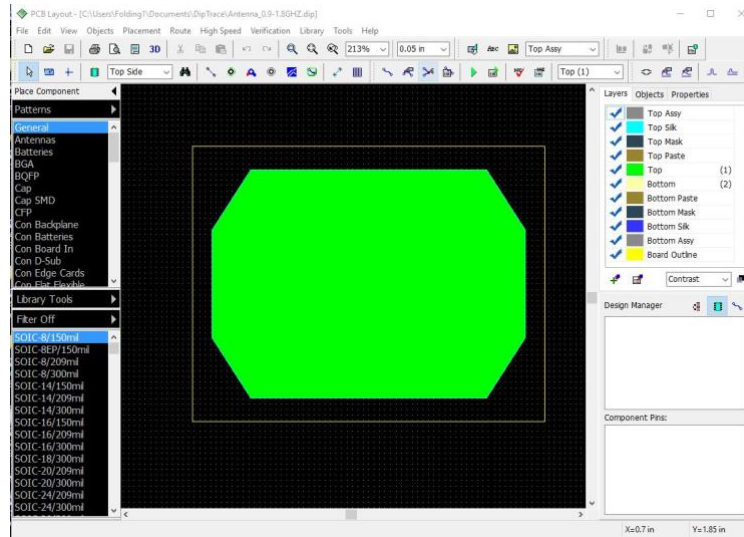
(a)
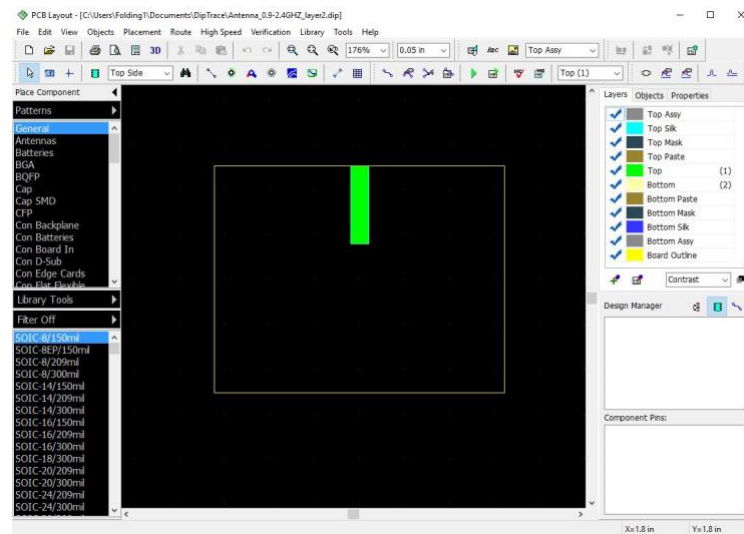
(b)

Figure 4.2 Dip Trace Software Windows.

4.2.2   LPKF ProtoMat S103

The LPKF ProtoMat S103 circuit board plotter for producing PCB prototypes and small batches is configured specifically for RF and microwave requirements. The touchless, pneumatic depth limiter further allows delicate surfaces, soft and flexible substrates to be processed. The ProtoMat S103 also carefully depanels irregular shaped flexible circuit boards from larger boards [19]. The ProtoMat S103 is extremely fast and accurate with a spindle speed of 100.000 rpm, a max. travel speed of 150 mm/s and a resolution of 0.5 μm. This ensures the accuracy required for

drilling and milling ultrafine structures especially for high-end applications in the RF and microwave field [19].

(a)   (b)
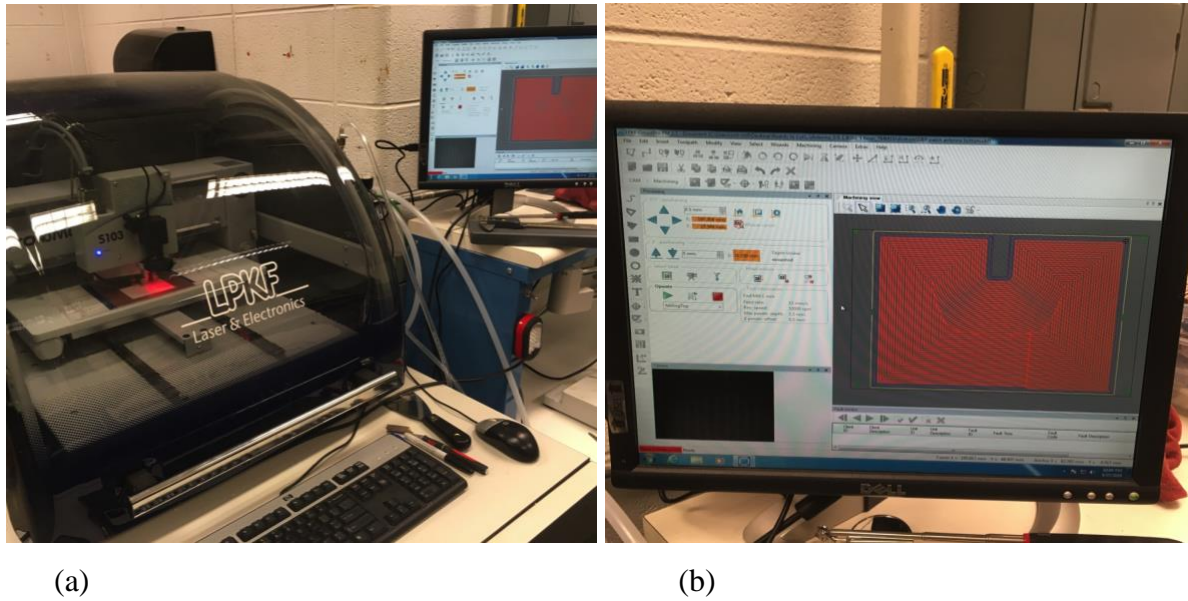
Figure 4.3 Cutting Machine & LPKF Software

4.3   Prototype Antennas

(a) Antenna 1 (0.9-1.8 GHz)   (b) Antenna 2 (0.9-2.4 GHz)
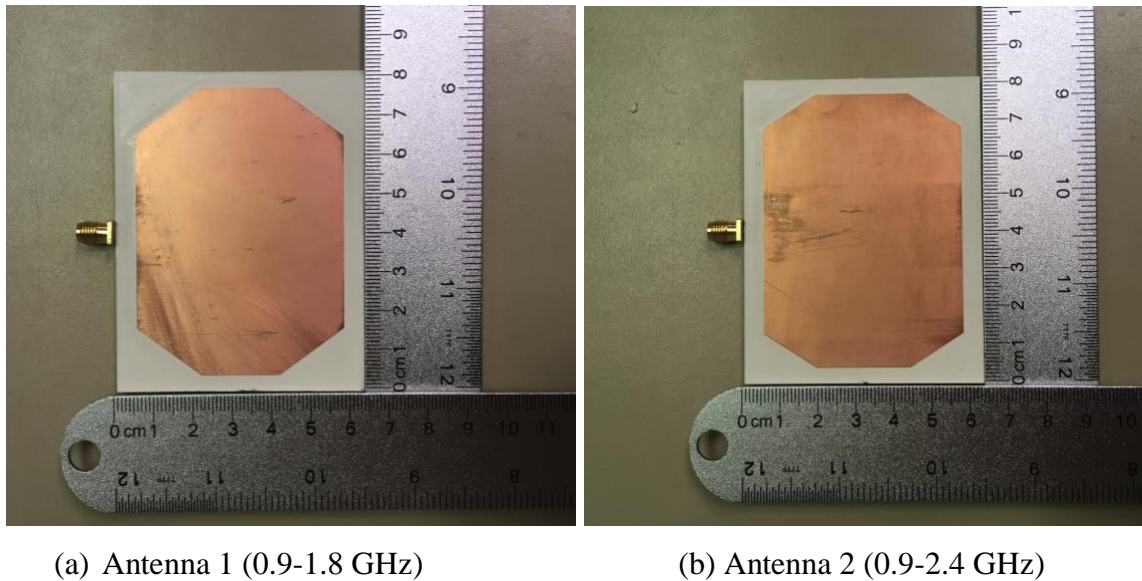
Figure 4.4 Prototypes Antennas

4.4   Antenna Structure

4.4.1   Top and Bottom Layers
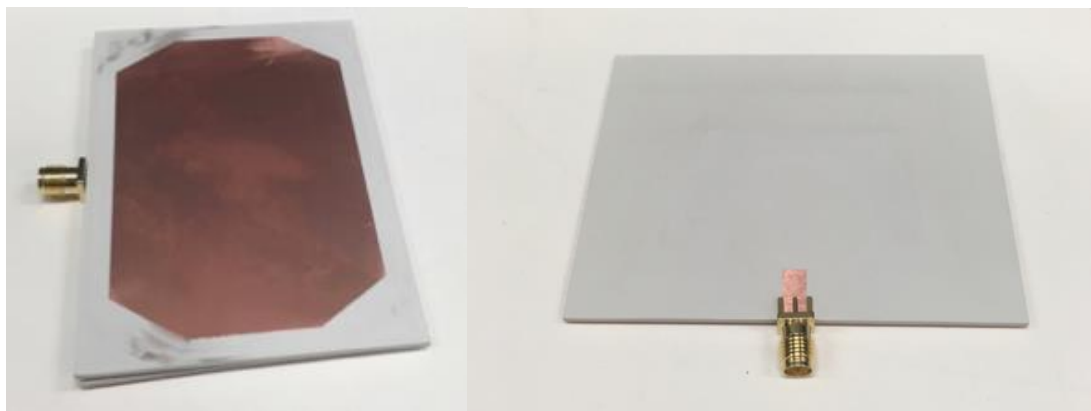
(a) Top layer   (b) Bottom layer

Figure 4.5 Antenna Layers

4.4.2   Dual Layer Substrate
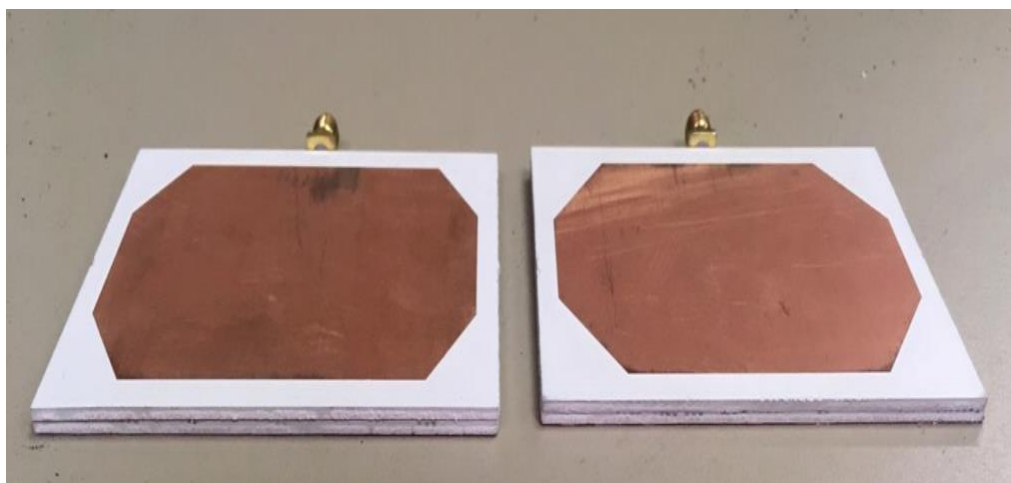
(b) Antenna 1   (b) Antenna 2

Figure 4.6 Dual Layer Substrate

4.4.3 Ground Plane Layer

(c) Antenna 1   (b) Antenna 2

Figure 4.7 Ground Plane Layers

5.   ANECHOIC CHAMBER & MEASUREMENTS

5.1   Anechoic Chamber

To provide a controlled environment, an all-weather capability, and security, and to minimize electromagnetic interference, indoor anechoic chambers have been developed as an alternative to outdoor testing. By this method, the testing is performed inside a chamber having walls that are covered with RF absorbers. The rectangular chamber [20] is usually designed to simulate free-space conditions and maximize the volume of the quiet zone. The design takes into account the pattern and location of the source, the frequency of operation, and it assumes that the receiving antenna at the test point is isotropic. Reflected energy is minimized by the use of high quality RF absorbers. Despite the use of RF absorbing material, significant specular reflections can occur, especially at large angles of incidence [5].
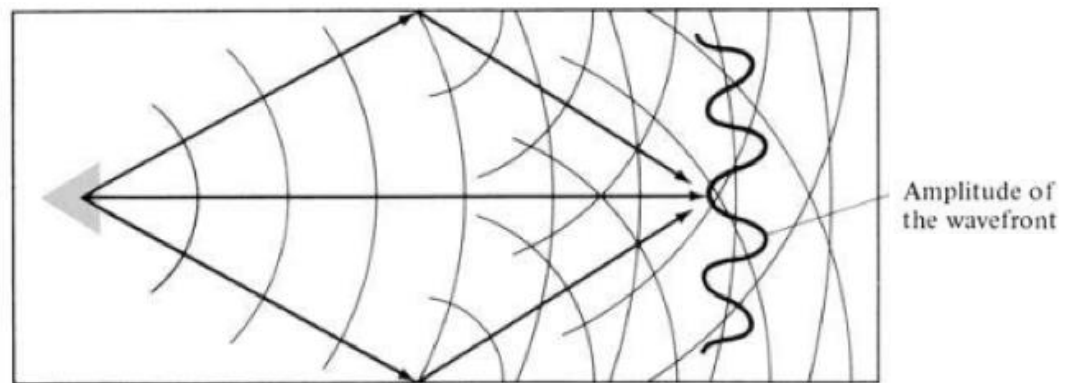
Figure 5.1 Rectangular Anechoic Chamber and the corresponding side wall specular reflections.

5.2   Far Field

The Far-Field measurements can be performed in outdoor or indoor ranges. In general, there are two basic types of Far-Field antenna ranges: reflection and free space ranges [22]. The one used for the measurements was the indoor anechoic chamber elevated range. In the free space ranges the reflections from the ground are minimized. Figure 5.3 shows the test setup.
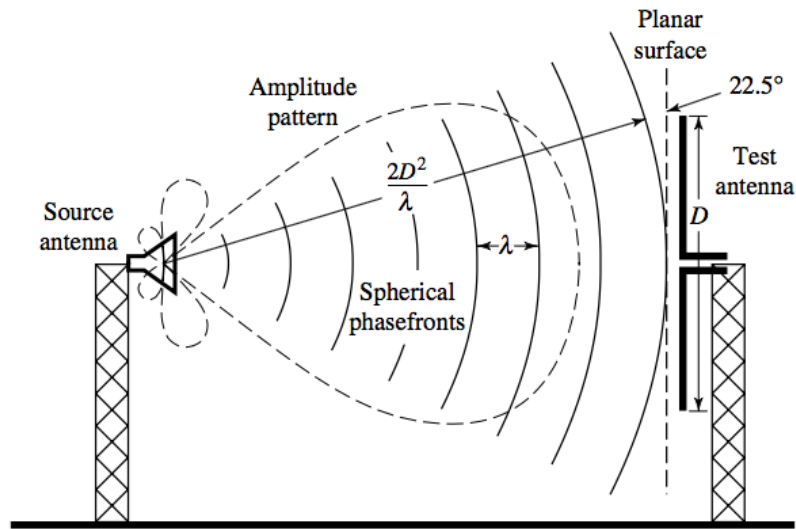
Figure 5.2 Far Field Region
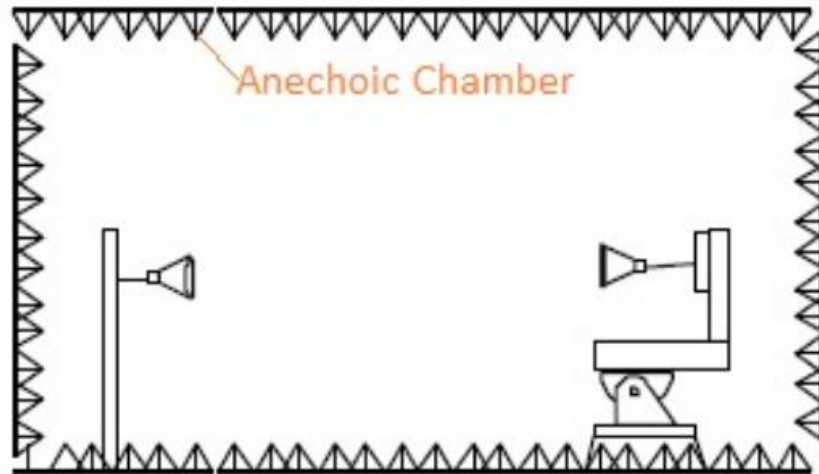
Figure 5.3 Indoor Far Field Antenna Test Range

5.3   Positioner and coordinate system

A practical way to obtain the radiation pattern is to record the signal received by the AUT through its motion in spherical coordinates (θ, φ), while keeping the probe antenna stationary [22]. Two orthogonal rotational axes are required in order to provide the relative motion of the AUT with respect to the source antenna. In the Elevation Over Azimuth positioner (EOA), the

elevation positioner provides the motion around the θ axis, while the azimuth positioner provides the motion around the Φ axis [22].
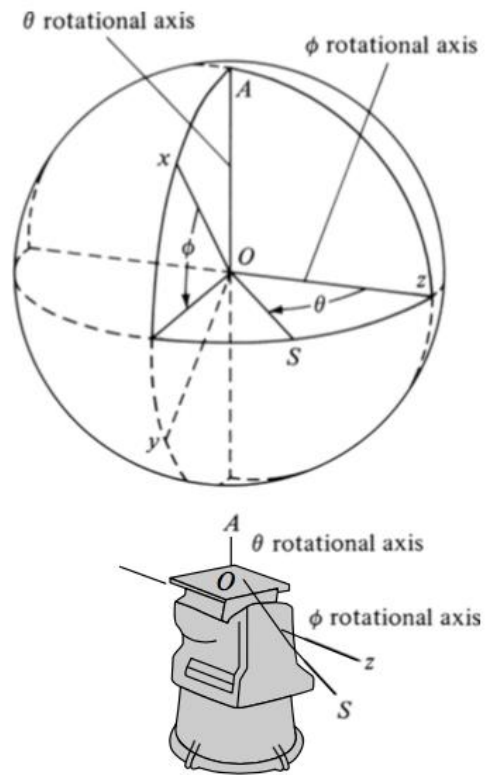
Figure 5.4 Elevation over Azimuth Positioner

5.4   Instrumentation Used for Measurement

The instrumentation used to accomplish the measuring tasks was selected to operate in a range of 300 MHz to 3.0 GHz. The following instrumentation were classified as [22]:

5.4.1 Antennas

5.4.1.1 Standard Calibrated Antenna

Figure 5.5 Log Periodic Aaronia HyperLog 7025

5.4.1.2 Reference Antenna
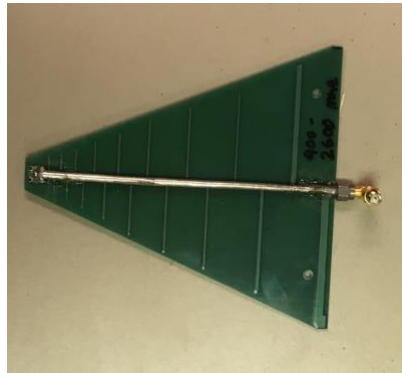
Figure 5.6 Log Periodic Kent Electronics WA5VJB

5.4.1.3 Antenna Under Test

Figure 5.7 AUT OMPA

5.4.2 Receiving System

5.4.2.1 Network Analyzer
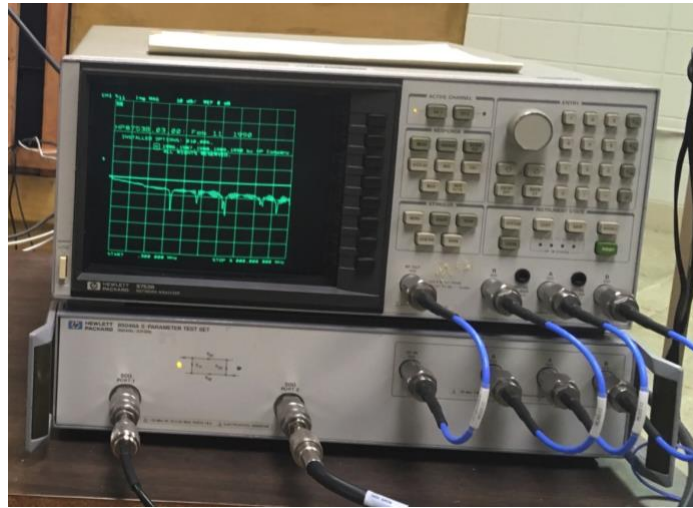
Figure 5.8 HP 8753B Network Analyzer with S-Parameters Ports

5.4.3 Positioning System

5.4.3.1 Elevation over Azimuth Positioner
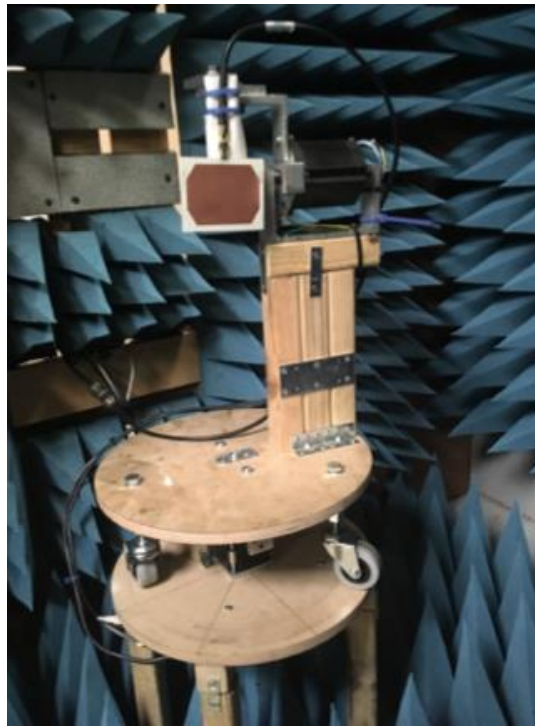
Figure 5.9 Antenna Positioner

5.4.4 Recording System

5.4.4.1 HP Computer
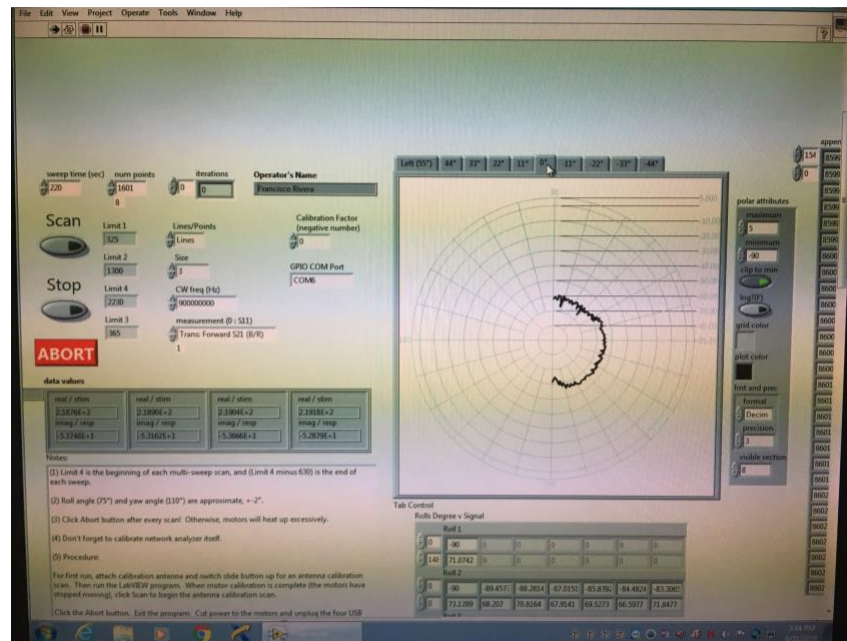
Figure 5.10 Lab View Software Window to Record the Radiations Pattern

5.5 Radiation Pattern Measurement

The patterns of antennas can be measured in transmit or receive mode. A two-dimensional pattern is referred to as a pattern cut. Pattern cuts can be obtained by fixing ϕ and varying θ (azimuth pattern) or fixing θ and varying ϕ (elevation pattern). To achieve the desired pattern cuts, the mounting structure of the system must have the capability to rotate in various planes. This can be accomplished by using different types of positioners such as Elevation-over Azimuth or Azimuth-over-Elevation mounts [22].

5.6 Gain Measurements

The method most commonly used to measure the gain of an antenna is the gain-transfer method. This technique utilizes a gain standard (with a known gain) to determine absolute gains. Initially relative gain measurements are performed, which when compared with the known gain of the standard antenna, yield absolute values. The method can be used with free-space and reflection

ranges, and for in situ measurements. The procedure requires two sets of measurements. In one set, using the test antenna as the receiving antenna, the received power (P_T) into a matched load is recorded. In the other set, the test antenna is replaced by the standard gain antenna and the received power (P_S) into a matched load is recorded. In both sets, the geometrical arrangement is maintained intact (other than replacing the receiving antennas), and the input power is maintained the same.

$$(G_{0t})_{dB} + (G_{or})_{dB} = 20log_{10}\left(\frac{4\pi R}{\lambda}\right) + 10log_{10}\left(\frac{P_r}{P_t}\right)$$

(35)

Where,

$(G_{0t})_{dB}=$ gain of transmitting antenna (dB)

$(G_{or})_{dB}=$ gain of the receiving antenna (dB)

$P_r=$ received power (W)

Writing two equations of the form of (), for free-space or reflection ranges, it can be shown that they reduce to [22]

$$(G_T)_{dB} = (G_S)_{dB} + 10log_{10}\left(\frac{P_T}{P_S}\right)$$

(36)

$$(G_T)_{dB} = (G_S)_{dB} + ((P_T)_{dB} - (P_S)_{dB})$$

(37)

Where $(G_T)_{dB}$ and $(G_S)_{dB}$ are the gains (in dB) of the test and standard gain antennas.

6. COMPARISON OF DATA SIMULATED & MEASURED

6.1 OMPA 900 MHz & 1.8 GHz (Antenna 1)

6.1.1 Return Loss (S11)

In the Figure 6.1 shows the comparison of the simulated and measured return loss (S11) of antenna 1 operating at 900 MHz and 1.8 GHz. The blue line is the simulated return loss (RL) and the red line the measured RL. The RL at 900 MHz for the simulated is -17.25 dB and for the measured is -21.8 dB. At 1.8 GHz the simulated RL is -20.37 dB and for the measured is -20.3 dB.
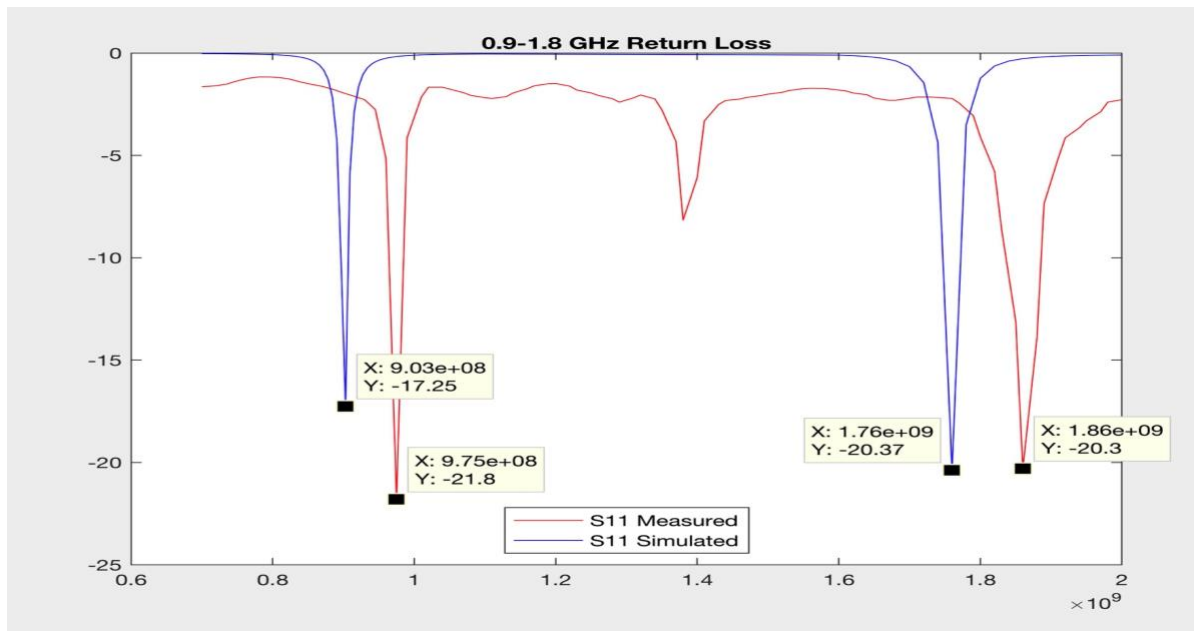
Figure 6.1 S-Parameter S11 Return Loss

6.1.2 Radiation Pattern 900 MHz at Vertical Polarization

The Figure 6.2 shows the comparison of the simulated and measured radiation pattern for the Octagonal Microstrip patch antenna. This measure is at 900 MHz for Vertical Polarization. The comparison shows similar pattern and magnitude.
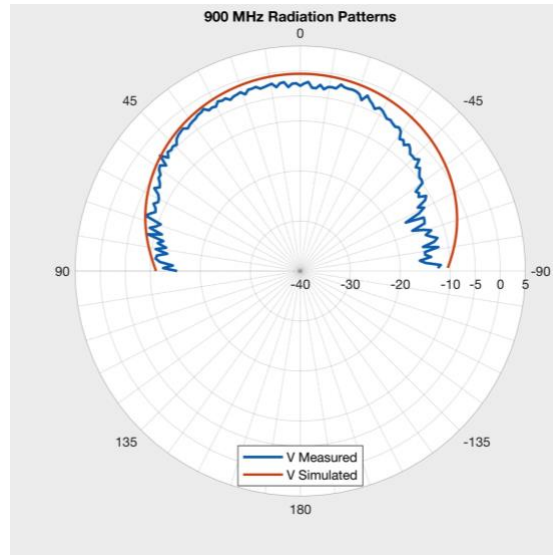
Figure 6.2 Radiation Pattern Comparison Simulated vs Measured

6.1.3 Radiation Pattern 900 MHz at Horizontal Polarization

The Figure 6.3 shows the comparison of the simulated and measured radiation pattern for the Octagonal Microstrip patch antenna. This measure is at 900 MHz for Horizontal Polarization. The comparison shows similar pattern and magnitude. A deep pattern can be found at -80 degrees and at 45 degrees the magnitude of the measured is less than the simulated.
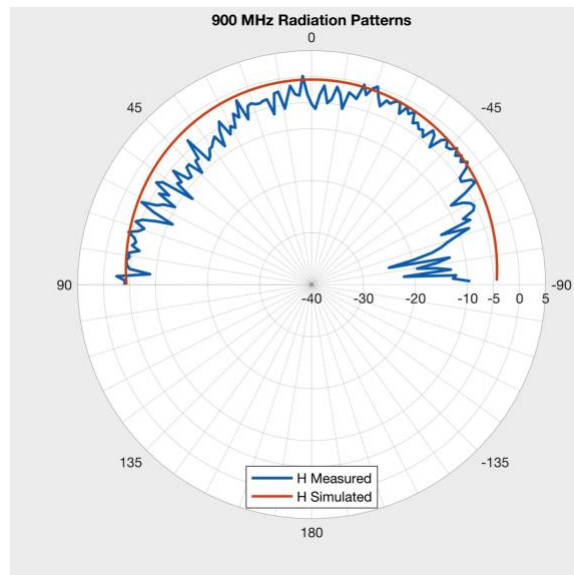
Figure 6.3 Radiation Pattern Comparison Simulated vs Measured

6.1.4   Radiation Pattern 1.8 GHz at Vertical Polarization

The Figure 6.4 shows the comparison of the simulated and measured radiation pattern for the Octagonal Microstrip patch antenna. This measure is at 1.8 GHz for Vertical Polarization. The comparison shows similar pattern. Similar magnitude can be seen from 90 degrees to 45 degrees. A relative difference in magnitude approximately of -5 dB can be seen from 39 degrees to -90 degrees.
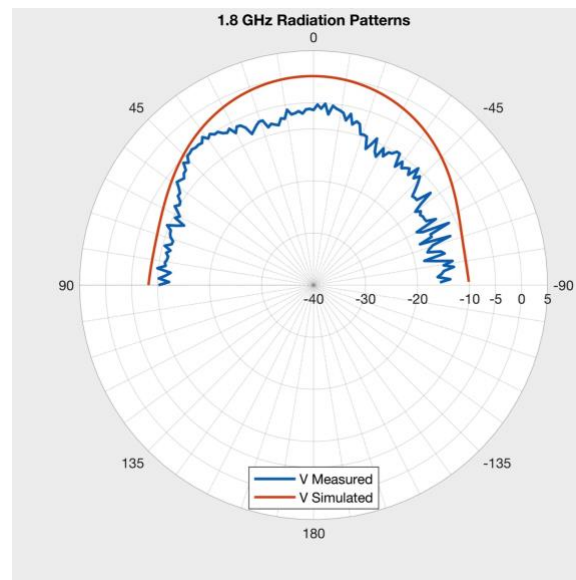
Figure 6.4 Radiation Pattern Comparison Simulated vs Measured

6.1.5   Radiation Pattern 1.8 GHz at Horizontal Polarization

The Figure 6.5 shows the comparison of the simulated and measured radiation pattern for the Octagonal Microstrip patch antenna. This measure is at 1.8 GHz for Horizontal Polarization. The comparison shows similar pattern. The magnitude of the measured was greater than the simulated.
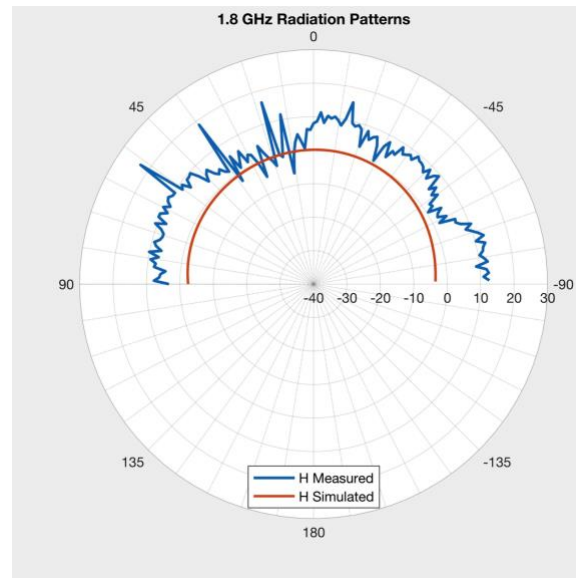
Figure 6.5 Radiation Pattern Comparison Simulated vs Measured

6.2   OMPA 900 MHz & 2.4 GHz (Antenna 2)

6.2.1   Return Loss (S11)
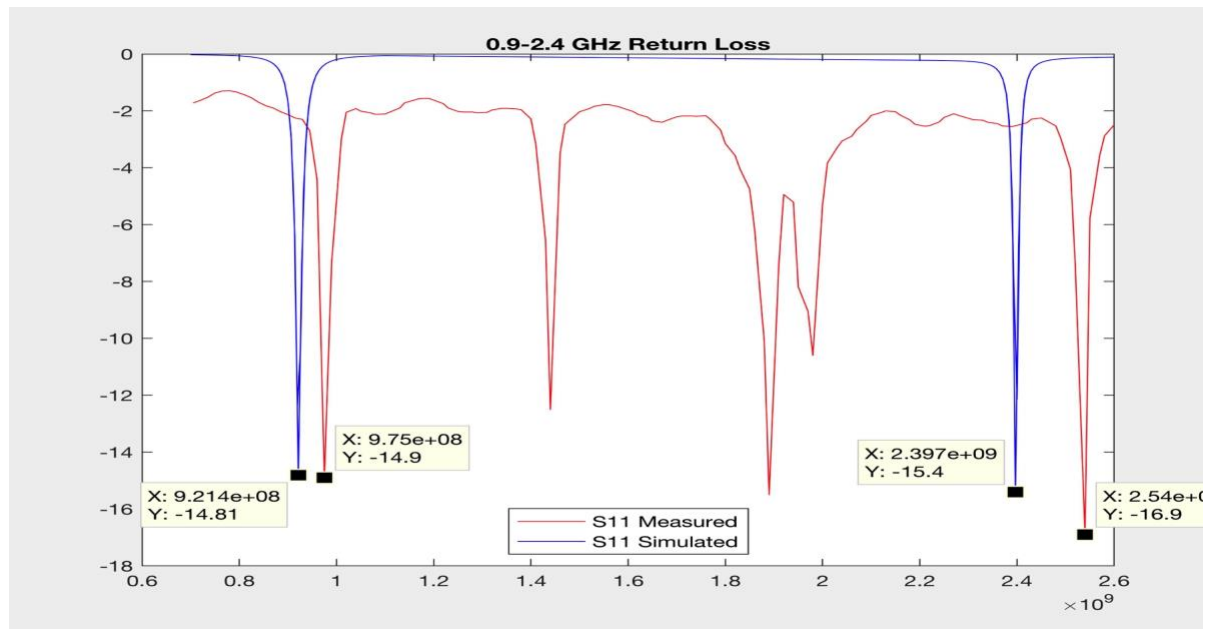
Figure 6.6 S-Parameter S11 Return Loss

In the Figure 6.6 above shows the comparison of the simulated and measured return loss (S11) of antenna 2 operating at 900 MHz and 2.4 GHz. The blue line is the simulated return loss (RL) and the red line the measured RL. The RL at 900 MHz for the simulated is -14.81 dB and for the measured is -14.9 dB. At 2.4 GHz the simulated RL is -15.4 dB and for the measured is -16.9 dB.

6.2.2 Radiation Pattern 900 MHz at Vertical Polarization

The Figure 6.7 shows the comparison of the simulated and measured radiation pattern for the Octagonal Microstrip patch antenna. This measure is at 900 MHz for Vertical Polarization. The comparison shows similar pattern. The measured radiation pattern is less than the magnitude of the simulated approximately by -10 dB.
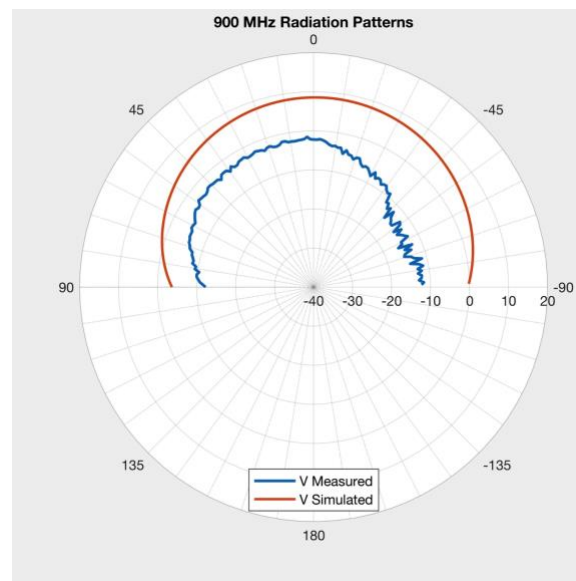
Figure 6.7 Radiation Pattern Comparison Simulated vs Measured

6.2.3 Radiation Pattern 900 MHz at Horizontal Polarization

The Figure 6.8 shows the comparison of the simulated and measured radiation pattern for the Octagonal Microstrip patch antenna. This measure is at 900 MHz for Horizontal Polarization. The comparison shows similar pattern. A deep pattern can be found at -80 degrees. The magnitude of the measured radiation pattern is less than the simulated approximately by 10dB.
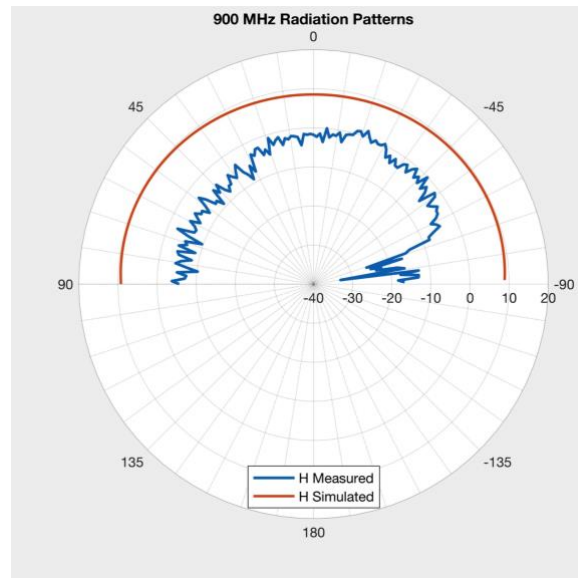
Figure 6.8 Radiation Pattern Comparison Simulated vs Measured

6.2.4 Radiation Pattern 2.4 GHz at Vertical Polarization

The Figure 6.9 shows the comparison of the simulated and measured radiation pattern for the Octagonal Microstrip Patch Antenna. This measure is at 2.4 GHz for Vertical Polarization. The comparison shows similar pattern. The magnitude of the measured is less than the simulated.
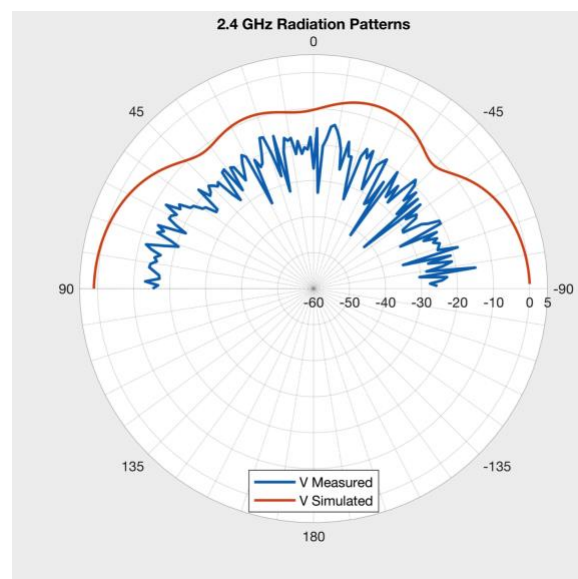
Figure 6.9 Radiation Pattern Comparison Simulated vs Measured

6.2.5 Radiation Pattern 2.4 GHz at Horizontal Polarization

The Figure 6.10 shows the comparison of the simulated and measured radiation pattern for the Octagonal Microstrip Patch Antenna. This measure is at 2.4 GHz for Horizontal Polarization. The comparison shows similar pattern and magnitude. The magnitude from 0 degree to -45 has a difference approximately of 5 dB.
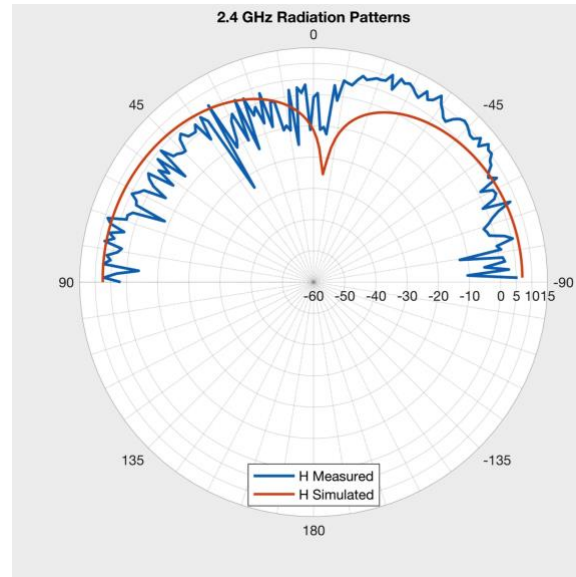
Figure 6.10 Radiation Pattern Comparison Simulated vs Measured

7. EXPERIMENT DESIGN & SETUP

7.1 Determine the objective of the study

The objective of this study is to identify if Antenna 1 is different to Antenna 2.

7.2 Obtain management and team approvals necessary for the study

In this case the objective is performed independently and approved by the committee advisor.

7.3 Determine the key inputs and/or outputs you will be monitoring
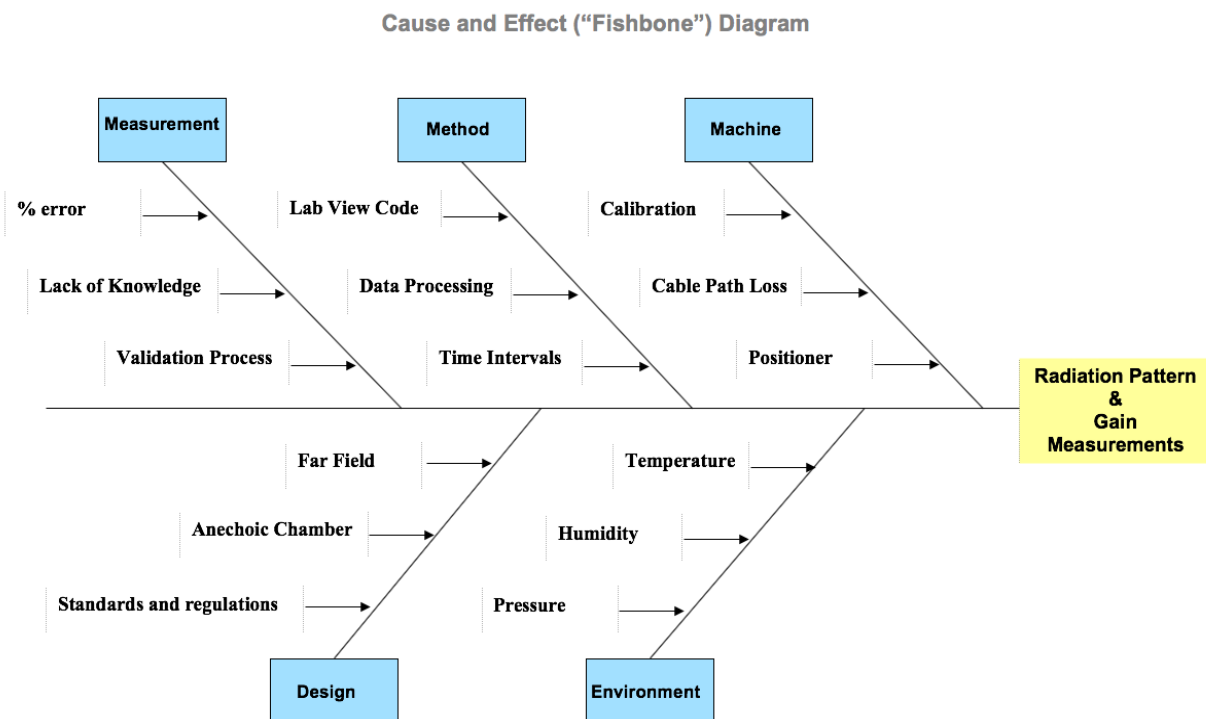
Figure 7.1 Fishbone Diagram

7.4 Ensure that the raw materials are available

Materials needed to perform the measurements:

- Anechoic Chamber

- Network Analyzer

- Elevation over Azimuth Positioner

- Type N and SMA RF Cables

- Computer

- Lab View Software

- Phidget Control Software

- Standard Calibrated Antenna

- Reference Antenna

- Antenna Under Test

- Calibration Kit

7.5   Make sure the measurement system is reliable

The required equipment complies with in the range of 300 MHz to 3 GHz. The measurements range is from 900MHz to 2.4 GHz meaning that the equipment is reliable to perform the experiments. The measurement process is call "Transfer Gain" or "Gain Comparison" more details can be found on Section 5.6. Before starting any experiment section, the equipment most be calibrated. For example, the Positioner must be calibrated by the software that receive the data. In the case of the network analyzer is most be calibrated using a calibration kit to calibrate the S-ports as open, close and short.

7.6   Define the standard process

If the experimental procedure is changed during the experiment all the data acquired will be invalidated. For that reason, always most follow the standard method to run the experiments. The following standard methods are to measure Radiation Pattern and Gain of the antenna.

Radiation Pattern and Gain Standard Measurement Method Process:
1. Turn on Network Analyzer and Computer. Make sure the 4 USB cables are connected to the computer (2 white USB are from the step motor controllers; one gray USB is from the positioner limits switch and one blue USB from network analyzer).
2. The reference antenna is connected to port 2 in the Network Analyzer.

3. The standard calibrated antenna is connected to Port 1 in the Network Analyzer.

4. Install the standard calibrated antenna in the positioner.

5. Close the Anechoic Chamber Door.

6. Turn on the Step motors.

7. Open the Lab View code named "Program".

8. Configure the frequency and type of measurement for example: S11 return loss, S21 gain or loss, etc.

9. After setting the parameters to measure, hit the "run command" on the upper left side of the program window and wait for the calibration of the positioner.

10. After the Calibration is done, Hit the "SCAN" button to run the measurement.

11. One time the measurement is done the data will be displayed on the screen and saved in a ".csv" file format for future data analysis. The Radiation pattern of the standard calibrated antenna is done.

12. For vertical and horizontal polarizations, the reference antenna at the end side of the anechoic chamber must be turn by 90 degrees.

13. Repeat steps 7 to 11 for different frequencies and measurements.

14. Open anechoic chamber to replace standard calibrated antenna with the antenna to test.

15. Repeat steps 5 to 11 for different frequencies and measurements.

16. Create a Excel file to paste the data of the radiation pattern of the standard calibrated antenna and the antenna under test. Use equation in section 5.6* to calculate the gain of the Antenna under test. *The Data of the standard calibrated gain is needed for the formula, you can find it in Appendix C.

17. Plot the radiation pattern and the Gain of the antenna under test.

7.7   Minimize any controllable sources of variation

Based on the standard method to measure the radiation pattern and gain there wasn't any sources of variations that can be eliminated or reduced.

7.8   Set the process to the best-known levels

These will be the measurement specifications for each experiment.

- Standard Calibrated Antenna
  - 900 MHz Vertical Polarization
  - 1.8 GHz Vertical Polarization
  - 2.4 GHz Vertical Polarization
  - 900 MHz Horizontal Polarization
  - 1.8 GHz Horizontal Polarization
  - 2.4 GHz Horizontal Polarization

- Antenna Under Test #1
  - 900 MHz Vertical Polarization
  - 1.8 GHz Vertical Polarization
  - 900 MHz Horizontal Polarization
  - 1.8 GHz Horizontal Polarization

- Antenna Under Test #2
  - 900 MHz Vertical Polarization
  - 2.4 GHz Vertical Polarization
  - 900 MHz Horizontal Polarization
  - 2.4 GHz Horizontal Polarization

7.9   Conduct a preliminary study

Sample size for a two-sided test null hypothesis $H_0: \mu_1 \neq \mu_2$

Sample size $n = 54$, based on $\alpha = 0.05$, $\beta = 0.2$, (Effect Size) $ES = \sigma/2$

7.10   Determine if the process is in control.

7.10.1 Calculate the process mean and process variation

Calculate the average process output (mean) and the scatter of all the data points in the sample around the mean (variation).

Process average output result = mean = $\bar{X}$

$$\bar{X} = \frac{(x1 + x2 + \cdots xn)}{n}$$

(38)

Spread of data around the mean = variance = S^2

$$S^2 = \frac{(x - \bar{X})^2}{n - 1}$$

(39)

7.10.2 Develop the appropriate Process Control Charts for your data

X-Bar and R Charts are for variables data. C and P Charts are for attribute data.

There could be two scenarios after examining the process output in this comparison:

A) The process meets the customer specification (all the data points are with the control limits and there is no increasing or decreasing trend of at least 7 data points) resulting in customer satisfaction.
B) The process does not meet the customer specifications (if either one or more than one data point is outside the control limits within the control chart.

7.10.3 Is the process in statistical control?

If Yes - Proceed to Step 11.

If No - Take the necessary steps to determine assignable causes of variation, then proceed to Step 12.

7.11 Compare the process output to the specifications

The process output is then compared to the required specifications given by the customers.

Determine the Process Capability Index (C_{pk}) (if not centered) or Ratio (C_p) (if centered).

$$C_{pk} = min\left[\frac{USL - \mu}{3\sigma}, \frac{\mu - LSL}{3\sigma},\right]$$

(40)

$$C_p = \frac{USL - LSL}{6\sigma}$$

(41)

7.12 Take action to control, improve and sustain process

In case the process output does not meet customer satisfaction, further action needs to be taken to bring the process into control. Further actions may include the use of fishbone diagrams to determine all the possible causes of variation / failure. A Control Plan defines the next actions to reduce or mitigate sources of variation and may include changes in procedures, changes in equipment, and mistake proofing.

What improvement actions does you recommend to bring the process in control?

8. CONCLUSION

In this thesis report two Octagonal Microstrip Patch Antennas using proximity coupling feed technique is given for Energy Harvesting. The first antenna design is for wireless communication GSM technology at 900 MHz and 1.8 GHz. The second antenna design is for wireless communication GSM and WIFI technologies at 900 MHz and 2.4 GHz. Both antennas designs have a double layer microstrip patch structure. The various antenna parameters like return loss, impedance, VSWR, radiation pattern and gain were studied. Also, the effects of physical parameters on the antenna were studied showing good agreement to improve the antenna performance. Various challenging occurs during the development of prototype and measuring. During the development of the prototype special cutting technic was needed to reduce the substrate from 4 mm to 1.6 mm of thickness. In the measuring process I designed a new positioner to measure the radiation patterns in a sweep of 180 degrees. Finally through a lot of the designs, simulations and measurements in a anechoic chamber the reasonable and good results have been obtained at dual frequencies of 900 MHz & 1.8 GHz and 900 MHz & 2.4 GHz.

APPENDIX A. MATLAB CODES

```matlab
%Francisco A. Rivera Abreu
%Microstrip Antenna Rectangular Patch
%MARP Calculator

clc
clear all
format long

disp('Design rectangular antenna by transmission line feeding using MATLAB');
disp('-----------------------------------------------------------------
----');

er = input('Enter the dielectric constant = ');
h = input('Enter the substrate thickness(in mm) = ');
f = input('Enter the frequency(in GHz) = ');
z = input('Enter the input impedance(ohm) = ');
disp('Calculating, Please Wait...');

f=f*1e9;

%Calculate the width
wid = (3e8/(2*f))*sqrt(2/(er+1))*1000;

%Calculate the Effective Dielectric Constant
e_eff = ((er+1)/2)+(((er-1)/2)*(1+((12*h)/wid))^-0.5);

%Calculate the Extension Length L
del_l = (((e_eff+0.3)*((wid/h)+0.264))/((e_eff -
0.258)*((wid/h)+0.8)))*(0.412*h);

%Calculate the Effective Length
l_eff = (3e8/(2*f*sqrt(e_eff)))*1000;

%Calculate the Actual Lentgh
L = l_eff-(2*del_l);

%Calculate the Conductance
la = (3e8/f)*1000;
k = (2*pi)/la;
x = k*wid;
il = -2+cos(x)+(x*sinint(x))+(sin(x)/x);
g1 = il/(120*pi*pi);

%Calculate the Mutual Conductance
a =
@(th)(((sin((x./2).*cos(th))./cos(th)).^2).*(besselj(0,(k.*L.*sin(th)))).*(si
n(th)).^ 3 );
a1 = integral(a,0,pi);
```

```matlab
g12 = a1/(120*pi*pi);


%Calculate the Input Impedance
r_in = 1/(2*(g1+g12));


%Calculate the insent feed point distance
inset = (L/pi)*(acos(sqrt(z/r_in)));


%Calculate minimum ground plane length
Lg_min = 6*h+L;


%Calculate minimum ground plane width
Wg_min = 6*h + wid;


%Calculate transmision line width
B = (377*pi)/(2*z*sqrt(er));
m1 = 2*B - 1;
m = log(m1);
n1 = B-1;
n = log(n1);
W = h*(2/pi)*(B-1-m+(((er-1)/(2*er))*(n+0.39*(0.61/er))));


%Calculate gap between path and tranmision line
g = (3e8*4.65e-9)/(sqrt(2*e_eff)*f*10^-9);


%Calculate gap Ratios
g1=W/10;
g2=W/15;
g3=W/20;
g4=W/25;
g5=W/30;
g6=W/35;
g7=W/40;


disp('Rectangular patch:')

disp(['The width of the patch(wp) is:',num2str(wid),'mm'])
disp(['The length of the patch(Lp)is:',num2str(L),'mm'])
disp(['The inset feed point(Fi)is:',num2str(inset),'mm'])
disp(['The width of the feed line(Wf)is:',num2str(W),'mm'])
disp(['The gap of the feed line(Gpf)is:',num2str(g),'mm'])
disp(['The minimum length of ground plane is:',num2str(Lg_min),'mm'])
disp(['The minimum width of ground plane is:',num2str(Wg_min),'mm'])



disp(['W/10 gap ratio is:',num2str(g1),'mm'])
disp(['W/15 gap ratio is:',num2str(g2),'mm'])
disp(['W/20 gap ratio is:',num2str(g3),'mm'])
disp(['W/25 gap ratio is:',num2str(g4),'mm'])
disp(['W/30 gap ratio is:',num2str(g5),'mm'])
disp(['W/35 gap ratio is:',num2str(g6),'mm'])
disp(['W/40 gap ratio is:',num2str(g7),'mm'])
```

```matlab
%Francisco A. Rivera Abreu
%Dual Band Octagonal Microstrip Patch Antenna
%Polar Plot Generator

pax = polaraxes;
N= 146; % divide [0,2pi] in N angle bins
dth = (pi)/N; % bin width
th =(0:N-1)*dth; % excludes th=0

polarplot(th,H2400_24,'LineWidth',2)
hold on
%hold (pax,'on')
polarplot(th,HS2400_24,'LineWidth',1.8)
% hold off
%hold (pax,'off')
t=title('2.4 GHz Radiation Patterns');
lgd=legend({'H Measured', 'H Simulated'},'FontSize',10);
set(0,'defaultfigurecolor',[0.94 0.94 0.94])
lgd.Location = 'south';
pax.ThetaZeroLocation = 'left';
pax.ThetaDir = 'clockwise';
pax.FontSize = 10;
pax.ThetaTick = [0 45 90 135 180 225 270 315];
pax.RLim = [-60 15];
pax.RAxisLocation = 180;
pax.ThetaTickLabel = {'90','45','0','-45','-90','-135','180','135'};
pax.RTick = [-60 -50 -40 -30 -20 -10 0 5 10 15];
pax.ThetaMinorGrid = 'on';
```

```matlab
%Francisco A. Rivera Abreu
%Dual Band Octagonal Microstrip Patch Antenna
%Rectangular Plot Generator for Return Loss

plot(X09_24,Y09_24,'red');
hold on
plot(X093_24,Y093_24,'blue');
t=title('0.9-2.4 GHz Return Loss');
lgd=legend({'S11 Measured','S11 Simulated'},'FontSize',10);
set(0,'defaultfigurecolor',[0.94 0.94 0.94])
lgd.Location = 'south';
```

APPENDIX B. DATA TRACKING GUIDE

PURDUE UNIVERSITY® FORT WAYNE

Anechoic Chamber LAB
Antenna Gain and Radiation Patterns Test
Department of Electrical and Computer Engineering
Francisco A. Rivera-Abreu
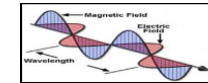
Completed	File name	Antenna	Frequency (MHz)	Polarization	Average Roll 0 degree (-dB)
	205517	Log-Periodic	900	H	56.63
	195447	Log-Periodic	900	V	46.61
	210155	Log-Periodic	975	H	56.84
	200246	Log-Periodic	975	V	42.15
	210831	Log-Periodic	1800	H	67.75
	201613	Log-Periodic	1800	V	45.15
	211457	Log-Periodic	1875	H	64.91
	202338	Log-Periodic	1875	V	48.00
	_024427	Log-Periodic	2400	H	68.37
	_023010	Log-Periodic	2400	V	46.56
	_025224	Log-Periodic	2534	H	65.02
	_023749	Log-Periodic	2534	V	47.79

Excel file Line #	
ROLL 1	9-157
ROLL 2	168-313
ROLL 3	324-469
ROLL 4	479-624
ROLL 5	635-780
ROLL 6	791-936
ROLL 7	946-1092
ROLL 8	1102-1247
ROLL 9	1258-1403
ROLL 10	1413-1559
Total Roll Po	1455

Co-Pol=Phi 0 degree
Cx-Pol=Phi 90 degree

Frequncy: 0.9-1.8

Completed	File name	Antenna	Frequency (MHz)	Polarization	Average Roll 0 degree (-dB)	Calibrated Antenna	AUT dB	Cal. Ant. Gain	AUT Gain dB
	233531	Rectangular Slot Patch	900	H	-62.93	56.63	-6.3	4.9	-1.4
	230137	Rectangular Slot Patch	900	V	-53.6	46.61	-6.99	4.9	-2.09
	234206	Rectangular Slot Patch	975	H	-52.93	56.84	3.91	4.9	8.81
	231029	Rectangular Slot Patch	975	V	-41.53	42.15	0.62	4.9	5.52
	234921	Rectangular Slot Patch	1800	H	-60.82	67.75	6.93	3.4	10.33
	231849	Rectangular Slot Patch	1800	V	-55.29	45.15	-10.14	3.4	-6.74
	235707	Rectangular Slot Patch	1875	H	-54.51	64.91	10.4	4.5	14.9
	232613	Rectangular Slot Patch	1875	V	-48.68	48.00	-0.68	4.5	3.82

Frequency:	0.9-2.4								
	Completed	File name	Antenna	equency (MH	Polarization	Average Roll 0 degree (-dB)	Calibrated Antenna	AUT dB	Cal. Ant. Gain	AUT Gain dB
		_001205	Rectangular Slot Patch	900	H	-61.88	56.63	-5.25	4.9	-0.35
	✔	_004121	Rectangular Slot Patch	900	V	-53.82	46.61	-7.21	4.9	-2.31
	✔	_001851	Rectangular Slot Patch	975	H	-53.27	56.84	3.57	4.9	8.47
	✔	_004815	Rectangular Slot Patch	975	V	-41.67	42.15	0.48	4.9	5.38
	✔	_002603	Rectangular Slot Patch	2400	H	-71.2	68.37	-2.83	4.5	1.67
	✔	_005639	Rectangular Slot Patch	2400	V	-68.31	46.56	-21.75	4.5	-17.25
	✔	_003244	Rectangular Slot Patch	2534	H	-59.81	65.02	5.21	4.4	9.61
	✔	_010319	Rectangular Slot Patch	2534	V	-56.95	47.79	-9.16	4.4	-4.76

Matlab Files Info:
Antenna #1 0.9-1.8 GHz
Antenna #2 0.9-2.4 GHz

Radiation Patterns Polar Plots Files Templates:	
MS900H18	Measured Pattern & Simulated Pattern 900Mhz Horizontal Pol. Antenna #1
MS900V18	Measured Pattern & Simulated Pattern 900Mhz Vertical Pol. Antenna #1
MS1800H18	Measured Pattern & Simulated Pattern 1.8 Ghz Horizontal Pol. Antenna #1
MS1800V18	Measured Pattern & Simulated Pattern 1.8 Ghz Vertical Pol. Antenna #1
MS900H24	Measured Pattern & Simulated Pattern 900Mhz Horizontal Pol. Antenna #2
MS900V24	Measured Pattern & Simulated Pattern 900Mhz Vertical Pol. Antenna #2
MS2400H24	Measured Pattern & Simulated Pattern 2.4 Ghz Horizontal Pol. Antenna #2
MS2400V24	Measured Pattern & Simulated Pattern 2.4 Ghz Vertical Pol. Antenna #2

Return Loss Linear Plot Files Templates:	
S11_0918	S-Parameter 11 Antenna #1
S11_09124	S-Parameter 11 Antenna #2

Matlab Polar Plot Data Variables Files:	
H900_18	Measured 900 Mhz Horizontal Pol. Antenna #1 Data
V900_18	Measured 900 Mhz Vertical Pol. Antenna #1 Data

H1800_18	Measured 1.8 Ghz Horizontal Pol. Antenna #1 Data
V1800_18	Measured 1.8 Ghz Vertical Pol. Antenna #1 Data
H900_24	Measured 900 Mhz Horizontal Pol. Antenna #2 Data
V900_24	Measured 900 Mhz Vertical Pol. Antenna #2 Data
H2400_24	Measured 2.4 Ghz Horizontal Pol. Antenna #2 Data
V2400_24	Measured 2.4 Ghz Vertical Pol. Antenna #2 Data
HS900_18	Simulated 900 Mhz Horizontal Pol. Antenna #1 Data
VS900_18	Simulated 900 Mhz Vertical Pol. Antenna #1 Data
HS1800_18	Simulated 1.8 Ghz Horizontal Pol. Antenna #1 Data
VS1800_18	Simulated 1.8 Ghz Vertical Pol. Antenna #1 Data
HS900_24	Simulated 900 Mhz Horizontal Pol. Antenna #2 Data
VS900_24	Simulated 900 Mhz Vertical Pol. Antenna #2 Data
HS2400_24	Simulated 2.4 Ghz Horizontal Pol. Antenna #2 Data
VS2400_24	Simulated 2.4 Ghz Vertical Pol. Antenna #2 Data

Matlab Return Loss Linear Plot Data Variables Files:

X09_18	Measured Antenna #1 X-axis Data
Y09_18	Measured Antenna #1 Y-axis Data
X093_18	Simulated Antenna #1 X-axis Data
Y093_18	Simulated Antenna #1 Y-axis Data
X09_24	Measured Antenna #2 X-axis Data
Y09_24	Measured Antenna #2 Y-axis Data
X093_24	Simulated Antenna #2 X-axis Data
Y093_24	Simulated Antenna #2 Y-axis Data

Matlab Workspaces

matlab.mat	
matlab2.mat	Contain all Variables in one file.

Matlab Rectangular Microstrip Antenna Calculator

MARP.m	Calculator for Rectangular Patch Parameters

APPENDIX C. STANDARD CALIBRATED ANTENNA CALIBRATION FILE

Frequency	**Gain dBi / (G(i)**	Gain dBd / G(D)	Antenna-Factor
700,000 MHz	**4.2**	2.05	22.99
710,000 MHz	**4.9**	2.75	22.42
720,000 MHz	**5.3**	3.15	22.14
730,000 MHz	**5.5**	3.35	22.06
740,000 MHz	**5.5**	3.35	22.17
750,000 MHz	**5.3**	3.15	22.49
760,000 MHz	**5**	2.85	22.91
770,000 MHz	**4.9**	2.75	23.12
780,000 MHz	**4.9**	2.75	23.23
790,000 MHz	**5.1**	2.95	23.14
800,000 MHz	**5.4**	3.25	22.95
810,000 MHz	**5.1**	2.95	23.36
820,000 MHz	**4.7**	2.55	23.87
830,000 MHz	**4**	1.85	24.67
840,000 MHz	**3.6**	1.45	25.18
850,000 MHz	**4**	1.85	24.88
860,000 MHz	**4.8**	2.65	24.18
870,000 MHz	**5.1**	2.95	23.98
880,000 MHz	**4.9**	2.75	24.28
890,000 MHz	**4.7**	2.55	24.58
900,000 MHz	**4.9**	2.75	24.47
910,000 MHz	**5.2**	3.05	24.27
920,000 MHz	**5.4**	3.25	24.17
930,000 MHz	**5.5**	3.35	24.16
940,000 MHz	**5.3**	3.15	24.45
950,000 MHz	**5**	2.85	24.84
960,000 MHz	**4.8**	2.65	25.14
970,000 MHz	**4.8**	2.65	25.23
980,000 MHz	**5**	2.85	25.11
990,000 MHz	**5.2**	3.05	25
1 GHz	**5.3**	3.15	24.99
1,01 GHz	**5.2**	3.05	25.18
1,02 GHz	**5**	2.85	25.46
1,03 GHz	**5**	2.85	25.55
1,04 GHz	**5.1**	2.95	25.53
1,05 GHz	**5.3**	3.15	25.41
1,06 GHz	**5.3**	3.15	25.5
1,07 GHz	**5.1**	2.95	25.78
1,08 GHz	**4.8**	2.65	26.16
1,09 GHz	**4.8**	2.65	26.24
1,1 GHz	**5**	2.85	26.12
1,11 GHz	**5.1**	2.95	26.1
1,12 GHz	**5**	2.85	26.27
1,13 GHz	**5**	2.85	26.35
1,14 GHz	**4.8**	2.65	26.63
1,15 GHz	**4.7**	2.55	26.8
1,16 GHz	**4.7**	2.55	26.88
1,17 GHz	**4.6**	2.45	27.05
1,18 GHz	**4.6**	2.45	27.13
1,19 GHz	**4.6**	2.45	27.2
1,2 GHz	**4.2**	2.05	27.67
1,21 GHz	**3.9**	1.75	28.05
1,22 GHz	**4**	1.85	28.02

1,23 GHz	**4.1**	1.95	27.99
1,24 GHz	**4.9**	2.75	27.26
1,25 GHz	**5**	2.85	27.23
1,26 GHz	**4.9**	2.75	27.4
1,27 GHz	**4.7**	2.55	27.67
1,28 GHz	**4.5**	2.35	27.93
1,29 GHz	**4.4**	2.25	28.1
1,3 GHz	**4.6**	2.45	27.97
1,31 GHz	**4.8**	2.65	27.84
1,32 GHz	**4.9**	2.75	27.8
1,33 GHz	**4.8**	2.65	27.97
1,34 GHz	**4.6**	2.45	28.23
1,35 GHz	**4.6**	2.45	28.3
1,36 GHz	**4.6**	2.45	28.36
1,37 GHz	**4.4**	2.25	28.62
1,38 GHz	**4.3**	2.15	28.79
1,39 GHz	**4.4**	2.25	28.75
1,4 GHz	**4.4**	2.25	28.81
1,41 GHz	**4.3**	2.15	28.97
1,42 GHz	**4.5**	2.35	28.84
1,43 GHz	**4.8**	2.65	28.6
1,44 GHz	**5**	2.85	28.46
1,45 GHz	**5**	2.85	28.52
1,46 GHz	**4.8**	2.65	28.78
1,47 GHz	**4.6**	2.45	29.04
1,48 GHz	**4.4**	2.25	29.3
1,49 GHz	**4.4**	2.25	29.35
1,5 GHz	**4.6**	2.45	29.21
1,51 GHz	**4.6**	2.45	29.27
1,52 GHz	**4.7**	2.55	29.23
1,53 GHz	**4.5**	2.35	29.48
1,54 GHz	**4.6**	2.45	29.44
1,55 GHz	**4.4**	2.25	29.7
1,56 GHz	**4.3**	2.15	29.85
1,57 GHz	**4.2**	2.05	30.01
1,58 GHz	**4.2**	2.05	30.06
1,59 GHz	**3.9**	1.75	30.42
1,6 GHz	**3.8**	1.65	30.57
1,61 GHz	**3.8**	1.65	30.63
1,62 GHz	**3.9**	1.75	30.58
1,63 GHz	**4.5**	2.35	30.03
1,64 GHz	**4.9**	2.75	29.69
1,65 GHz	**5**	2.85	29.64
1,66 GHz	**4.8**	2.65	29.89
1,67 GHz	**4.6**	2.45	30.14
1,68 GHz	**4.5**	2.35	30.3
1,69 GHz	**4.5**	2.35	30.35
1,7 GHz	**4.6**	2.45	30.3
1,71 GHz	**4.7**	2.55	30.25
1,72 GHz	**4.7**	2.55	30.3
1,73 GHz	**4.5**	2.35	30.55
1,74 GHz	**4.4**	2.25	30.7
1,75 GHz	**4.5**	2.35	30.65
1,76 GHz	**4.7**	2.55	30.5

1,77 GHz	**4.7**	2.55	30.55
1,78 GHz	**4.3**	2.15	31
1,79 GHz	**3.8**	1.65	31.55
1,8 GHz	**3.4**	1.25	32
1,81 GHz	**3.4**	1.25	32.04
1,82 GHz	**3.5**	1.35	31.99
1,83 GHz	**3.6**	1.45	31.94
1,84 GHz	**3.8**	1.65	31.79
1,85 GHz	**4.3**	2.15	31.33
1,86 GHz	**4.5**	2.35	31.18
1,87 GHz	**4.5**	2.35	31.23
1,88 GHz	**4.5**	2.35	31.27
1,89 GHz	**4.7**	2.55	31.12
1,9 GHz	**4.7**	2.55	31.17
1,91 GHz	**4.7**	2.55	31.21
1,92 GHz	**4.5**	2.35	31.46
1,93 GHz	**4.1**	1.95	31.9
1,94 GHz	**4.1**	1.95	31.95
1,95 GHz	**4.4**	2.25	31.69
1,96 GHz	**4.6**	2.45	31.54
1,97 GHz	**4.8**	2.65	31.38
1,98 GHz	**4.7**	2.55	31.52
1,99 GHz	**4.5**	2.35	31.77
2 GHz	**4.2**	2.05	32.11
2,01 GHz	**4.2**	2.05	32.15
2,02 GHz	**4.3**	2.15	32.1
2,03 GHz	**4.4**	2.25	32.04
2,04 GHz	**4.5**	2.35	31.98
2,05 GHz	**4.5**	2.35	32.03
2,06 GHz	**4.4**	2.25	32.17
2,07 GHz	**4.4**	2.25	32.21
2,08 GHz	**4.4**	2.25	32.25
2,09 GHz	**4.6**	2.45	32.09
2,1 GHz	**4.7**	2.55	32.03
2,11 GHz	**4.7**	2.55	32.08
2,12 GHz	**4.5**	2.35	32.32
2,13 GHz	**4.4**	2.25	32.46
2,14 GHz	**4.5**	2.35	32.4
2,15 GHz	**4.7**	2.55	32.24
2,16 GHz	**4.9**	2.75	32.08
2,17 GHz	**4.9**	2.75	32.12
2,18 GHz	**4.7**	2.55	32.36
2,19 GHz	**4.5**	2.35	32.6
2,2 GHz	**4.4**	2.25	32.74
2,21 GHz	**4.4**	2.25	32.78
2,22 GHz	**4.6**	2.45	32.62
2,23 GHz	**4.5**	2.35	32.76
2,24 GHz	**4.5**	2.35	32.79
2,25 GHz	**4.3**	2.15	33.03
2,26 GHz	**4.3**	2.15	33.07
2,27 GHz	**4.3**	2.15	33.11
2,28 GHz	**4.3**	2.15	33.15
2,29 GHz	**4.5**	2.35	32.99
2,3 GHz	**4.3**	2.15	33.22

2,31 GHz	**4.2**	2.05	33.36
2,32 GHz	**4**	1.85	33.6
2,33 GHz	**4**	1.85	33.64
2,34 GHz	**4.2**	2.05	33.47
2,35 GHz	**4.4**	2.25	33.31
2,36 GHz	**4.5**	2.35	33.25
2,37 GHz	**4.5**	2.35	33.28
2,38 GHz	**4.5**	2.35	33.32
2,39 GHz	**4.4**	2.25	33.46
2,4 GHz	**4.5**	2.35	33.39
2,41 GHz	**4.5**	2.35	33.43
2,42 GHz	**4.5**	2.35	33.47
2,43 GHz	**4.4**	2.25	33.6
2,44 GHz	**4.3**	2.15	33.74
2,45 GHz	**4.2**	2.05	33.87
2,46 GHz	**4.2**	2.05	33.91
2,47 GHz	**4.4**	2.25	33.74
2,48 GHz	**4.5**	2.35	33.68
2,49 GHz	**4.7**	2.55	33.51
2,5 GHz	**4.4**	2.25	33.85

REFERENCES

[1]   Collado and A. Georgiadis, "Conformal hybrid solar and electro- magnetic (EM) energy harvesting rectenna," *IEEE Trans. Circuits Syst.*, vol. 60, no. 8, pp. 2225–2234, Aug. 2013.

[2]   W. Tu, S. Hsu, and K. Chang, "Compact 5.8-GHz rectenna using stepped- impedance dipole antenna," *IEEE Antennas Wireless Propag. Lett.*, vol. 6, pp. 282–284, 2007.

[3]   M. Arrawatia, M. S. Baghini, and G. Kumar, "Broadband bent triangu- lar omnidirectional antenna for RF energy harvesting," *IEEE Antennas Wireless Propag. Lett.*, vol. 15, pp. 36–39, 2016.

[4]   Krikidis, S. Timotheou, S. Nikolaou, G. Zheng, D. W. Kwan, and R. Schober, "Simultaneous wireless information and power transfer in modern communication systems," *IEEE Commun. Mag.*, vol. 52, no. 11, pp. 104–110, Nov. 2014.

[5]   C. A. Balanis, "Microstrip antennas," in *Antenna Theory Analysis and Design*, 3rd ed. Hoboken, NJ, USA: Wiley, 2005.

[6]   Binu Paul, S. Mridula, C. K. Aanandan, and P. Mohanan, "Conformal FDTD analysis of an Octagonal Microstrip Patch antenna"; pp. 5259-5262, 2007 IEEE

[7]   David M. Pozar, "Microstrip Antennas", *Proceedings of IEEE*, Vol. 80, No.1, January 1992

[8]   Indra Surjati, "Dual Frequency Operation Triangular Microstrip Antenna Using A Pair of Slit," *2005 Asia-Pacific Conference on communications,* Perth Western Australia, 3-5, pp. 124-126, October 2005

[9]   C. L. Tang, H. T. Chen, and K. L. Wong, "Small circular microstrip antenna with dual-frequency operation," *IEEE Electron. Lett,* vol. 33, no. 13, pp. 1112-1113, Jun. 1997

[10]   K. L. Wong and W. S. Chen, "Compact microstrip antenna with dual frequency operation," *IEEE Electron. Lett,* vol. 33, no. 8, pp. 646-647, Apr. 1997

[11]   S. C. Pan and K. L. Wand, "Dual frequency triangular microstrip antenna with shorting pin," *IEEE Trans. Antennas Propag,* vol.45, no. 12, pp. 1889-1891, Dec. 1997

[12] S. Maci, G. B. Gentili, P. Piazzesi, and C. Salvador, "Dual band slot loaded patch antenna," *Proc. Inst. Elect Eng. Microw.* Antennas Propag, vol. 142, no. 3, pp. 225-232, Jun. 1995

[13] B. F. Wang and Y. T. Lo, "Microstrip antennas for dual-frequency operation," *IEEE Trans Antennas Propag,* vol. 32, no. 9, pp. 938-943, Sep. 1984

[14] J. F. Zurcher, A. Skrivervik, O. Staub, and S. Vaccaro, "A compact dual-port dual-frequency printed antenna with high decoupling," *Microw Opt. Technol Lett,* vol. 19, no. 2, pp. 131-137, Oct. 1998

[15] D.M. Pozar, "A microstrip antenna aperture coupled to a microstrip line," *Electron Lett* , vol. 21, no. 2, pp. 49-50, 1985

[16] Randy Bancroft Microstrip Antenna, "The Analysis and Design of Microstrip Antennas and Arrays", Second Edition, 1995.

[17] Balanis, C.A., "Antenna Theory Analysis and Design", 4th Edition. New Jersey, John Wiley and Sons, 2005.

[18] Garg, R., Bhartia, P. and Ittipiboon, A., "Microstrip Antenna Design handbook Boston: Artech, House",2001.

[19] https://www.lpkf.com/products/rapid-pcb-prototyping/circuit-board-plotter/protomat-s103.htm

[20] M. R. Gillette and P. R. Wu, "RF Anechoic Chamber Design Using Ray Tracing," *1977 Int. IEEE/AP-S Symp. Dig.*, pp. 246–252, June 1977.

[21] W. H. Kummer and E. S. Gillespie, "Antenna Measurements—1978," *Proc. IEEE*, Vol. 66, No. 4, pp. 483–507, April 1978. © (1978) IEEE

[22] ANSI/IEEE Standard Test Procedures for Antennas, ANSI/IEEE Std. 149-1979, IEEE, New York; John Wiley Distributors.

[23] Antennas from Theory to Practice/ Yi. Huang and K. Boyle, John Wiley & sons 2008, ISBN 978-0-470-51028-5

PUBLICATION

- F. Rivera and A. Eroglu, "Dual Band Octagonal Microstrip Antenna Design Method for Energy Harvesting," 2018 IEEE International Symposium on Antennas and Propagation and USNC-URSI Radio Science Meeting, Boston, MA, USA.